JPL PUBLICATION 78-102

Color Enhancement of Landsat Agricultural Imagery

Final Report for the JPL LACIE Image Processing Support Task

Daryl P. Madura
James M. Soha
William B. Green
David B. Wherry
Stanley D. Lewis

December 15, 1978

National Aeronautics and Space Administration

Jet Propulsion Laboratory
California Institute of Technology
Pasadena, California

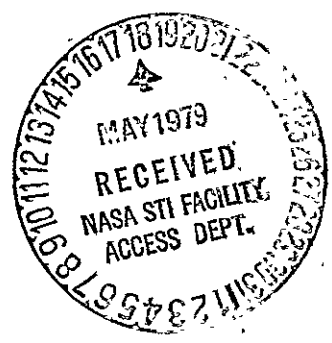

JPL PUBLICATION 78-102

Color Enhancement of Landsat Agricultural Imagery

Final Report for the JPL LACIE Image Processing Support Task

Daryl P. Madura
James M. Soha
William B. Green
David B. Wherry
Stanley D. Lewis

December 15, 1978

National Aeronautics and
Space Administration

Jet Propulsion Laboratory
California Institute of Technology
Pasadena, California

The research described in this publication was carried out by the Jet Propulsion Laboratory, California Institute of Technology, under NASA Contract No NAS7-100

PREFACE

The work described in this report was performed by the Observational Systems Division of the Jet Propulsion Laboratory.

ACKNOWLEDGEMENTS

The assistance provided by Jim Derbonne of the Earth Resources Program office at Johnson Space Center in defining the tasks described in this report and in obtaining the necessary funding is gratefully acknowledged. The technical assistance provided at JSC by Jim Sulester, Lew Wade, Richard Juday, Wes Palmer, and Bob Payne was very much appreciated. We would especially like to thank Mike Wolf and Ed Armstrong of the IPL color laser film recording facility and John Hewitt, Dave Deats, Kevin Mendelsohn, and Sadr Mohsenin of the JPL Photo Lab for the expedient generation and processing of the color film products.

CONTENTS

FIGURES

FIGURES (Cont.)

TABLES

1. INTRODUCTION

1.1 BACKGROUND

The directors of the Johnson Space Center and the Jet Propulsion Laboratory met during 1977 to explore areas of joint effort that might be beneficial to both institutions. One area that was identified as a potential area for cooperative effort was image processing. Discussions were initiated between Mr. Gene Rice, head of the Earth Resources Program Office (ERPO) at JSC, and Mr. William Green, manager of the Science Data Analysis Section at JPL, which includes the Image Processing Laboratory (IPL). After a series of meetings between JSC and JPL personnel, the activity described in this report was defined and funded, and the task was initiated at JPL in March 1978. The study was performed during the seven month period from March to September 1978, at a total cost of $50,000. The funding allocation also provided IPL support to a JSC/Mitre Corp. study of future computing requirements for NASA's Earth Resources Program.

At JPL, the task was monitored by Jim Soha, supervisor of the Geology Applications Group, and at JSC, by Jim Derbonne of the Earth Resources Program Office. Technical coordination at JSC was provided by Don Hay, Jim Sulester, and John Lyons.

Timely performance on this task was possible because of the support provided by IPL's color laser film recording facility, under the direction of Mike Wolf, and by the JPL Photo Lab managed by John Hewitt.

1.2 PURPOSE AND OBJECTIVES

The purpose of this study was to determine if multispectral image processing techniques developed at the Jet Propulsion Laboratory's Image Processing Laboratory (IPL) for mineral exploration applications could be beneficially applied to the analysis of LACIE agricultural data. Landsat multispectral imagery provides the main source of data for both applications.

In the past year, a decorrelation enhancement procedure employing the principal component transformation has been successfully used at JPL to increase substantially the discriminability of geologic formations in color composites of Landsat imagery. The transformation is employed to introduce greater color into scenes by more fully utilizing the range of the color domain. A complete description of the decorrelation procedure and its application to the enhancement of

color differences is given in the next section.

The main thrust of this study was to utilize the decorrelation procedure in the enhancement of LACIE data. At the outset, the main issue to be addressed was whether or not the introduction of more color into LACIE imagery by this technique increased the discrimination between wheat and non-wheat areas. The analysis logically led to the identification of the following additional issues for evaluation:

1. The degree of color consistency remaining between acquisitions of a given test site after the process of increasing the color range via the decorrelation technique.
2. The effect of the intrinsic noise in the data on the end products and the development of techniques to effectively deal with the noise.
3. The potential for multicrop analysis resulting from greater color discriminability.

Section Three defines the various processing techniques employed in the attempt to deal with the above issues. Section Four discusses the motivation behind each of the processing techniques and gives a preliminary evaluation of the resulting products.

1.3 OVERVIEW OF PROCESSING

The data base used in this study was made up of 12 LACIE test sites (segments). Each segment was composed of from 4 to 13 separate acquisitions. The total data base is summarized in Table 1.1. The total number of acquisitions for the entire data base was 92. Occasionally, within a segment, a pair of acquisitions were obtained such that they differed in time by only one day. In this study only one acquisition of such a pair was used in the analysis. The remaining acquisitions (81 in all) formed the working data set. The omitted acquisitions are followed by an asterisk in Table 1.1. Each segment is characterized by (1) LACIE segment number, (2) location by latitude and longitude, (3) verbal description of location, e.g., western Kansas, and (4) a list of acquisitions. Each acquisition is denoted by a five digit number code. The first two digits represent the year in which the acquisition was made. The last three digits indicate the Julian day.

Virtually all processing involved adapting the decorrelation enhancement technique to the LACIE application. Several variations of the method were

investigated. Both linear and non-linear enhancement techniques were applied. The use of filtering to reduce the effects of random noise was explored. Normalization of images to deal with the effects of solar illumination angle and atmospheric path length was also investigated.

Generally, a particular processing technique was first applied to a few selected individual acquisitions. If the results seemed promising, the technique was then applied to a larger portion of the working data set - typically a segment or two. Certain techniques were eventually applied to all acquisitions of the working data set to permit a comprehensive evaluation. Table 3.3 in Section Three summarizes the extent of the processing performed in this study.

Photographic prints of all processed products are presented in a supplemental volume. Copies of the supplement exist at the Earth Resources Program Office and the office of Don Hay at JSC, and at the Image Processing Laboratory at JPL [contact Jim Soha, (213)354-2722]. A very limited number of examples are reproduced in this volume.

TABLE 1.1 DATA BASE

SEGMENT 1000

N040-34/W102-54 Northeastern Colorado

76255	76310	76328	76363	77052
77142	77159*	77160	77177*	77178
77196	77213*	77214		

SEGMENT 1183

N037-34/W095-27 Southeastern Kansas

76285	76340	76358	77028	77046
77063*	77064	77081*	77082	77099
77118	77153	77154*		

SEGMENT 1531

N048-14/W108-16 Northern Montana

76279	76315	77112	77129	77147*
77148	77184	77220		

SEGMENT 1537

N047-27/W105-30 Western Montana

76349	77091	77127	77181

SEGMENT 1606

N048-16/W101-22 Northern N. Dakota

77125	77143	77179	77197	77250

SEGMENT 1625

N047-16/W102-33 Western N. Dakota

77125	77143	77179	77197	77233

SEGMENT 1637

N047-15/W099-19 Central N. Dakota

77123	77140	77159	77194	77248

SEGMENT 1648

N046-04/ W103-06 Southwestern N. Dakota

77107	77125	77143	77179	

SEGMENT 1734

N048-19/W110-42 Northern Montana

76245	76263	76281	77059	77095
77113	77203			

SEGMENT 1739

N047-45/ W111-30 Northern Montana

76281*	76282	77113*	77114	77131*
77132	77149*	77150	77168	77222

SEGMENT 9930

N037-15/W098-30 Southern Kansas

76287	76306	76323	76360	77011
77029	77048	77066	77083	77156
77191				

SEGMENT 9931

N048-32/W109-19 Northern Montana

76316	76352	77058	77112	77148
77184	77220			

*acquisitions omitted from working data set.

2. DECORRELATION ENHANCEMENT TECHNIQUES

The basic objective chosen for this task was to introduce greater color variation into processed LACIE segments, hopefully aiding in the discrimination of crop information. The underlying reason for the rather poor range of color content found in many Landsat color composites is the high degree of correlation between the image data sensed in the Landsat spectral bands. The standard approach of applying contrast enhancements to each of the spectral bands prior to producing a color display does not remove this interband correlation. Figure 2.1 illustrates schematically, in terms of a 3-dimensional histogram, why correlation between bands limits color range. Each image element in a Landsat color composite corresponds to a point in histogram space determined by the blue, green, and red coordinate values (in most cases, blue, green, and red correspond to Landsat channels 4, 5, and 7 respectively). Interband correlation forces most image elements to lie in a long narrow region of histogram space near the achromatic axis. Even after contrast enhancement of individual components, there are substantial regions of histogram space which are underutilized. These underutilized areas represent unused color range. Figure 2.2 provides a 2-dimensional illustration of the problem for a sample LACIE segment.

Fortunately a procedure exists for removing correlation from multispectral image components. The principal component, or Karhunen-Loeve, transformation has seen widespread use in remote sensing applications. Briefly, each picture element of an n component multispectral scene is regarded as a sample vector from an n-dimensional random process. An nxn covariance matrix C for the process is estimated [$C=E\{(x-E\{x\})(x-E\{x\})^T\}$ where x is a multispectral image vector and $E\{.\}$ denotes expectation] using a subset of image elements. Then an n-dimensional rotation which diagonalizes the covariance matrix is applied to each picture element in the scene. Since the new covariance matrix is diagonal, no correlation exists between the new, rotated components. The rotation matrix is composed of the n eigenvectors of the original covariance matrix. Any three of the resulting principal components can be individually contrast enhanced and then color composited for display. Since the individual components are uncorrelated, such a display will generally evidence a full range of color.

The principal components, however, are not the only set of coordinate axes available for obtaining a transformed set of uncorrelated image components. If

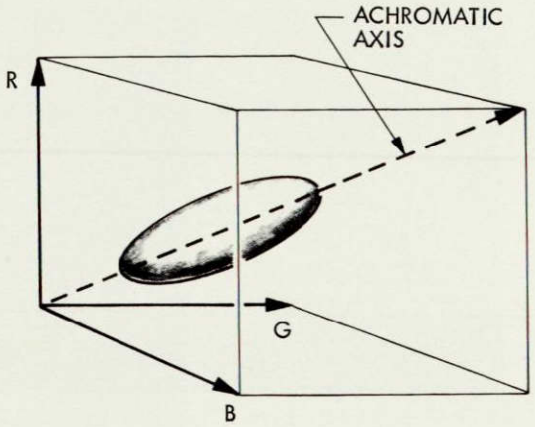

Figure 2.1(a) Correlation between components causes the 3-dimensional histogram of a typical color image to assume an elongated shape, generally centered near the achromatic axis.

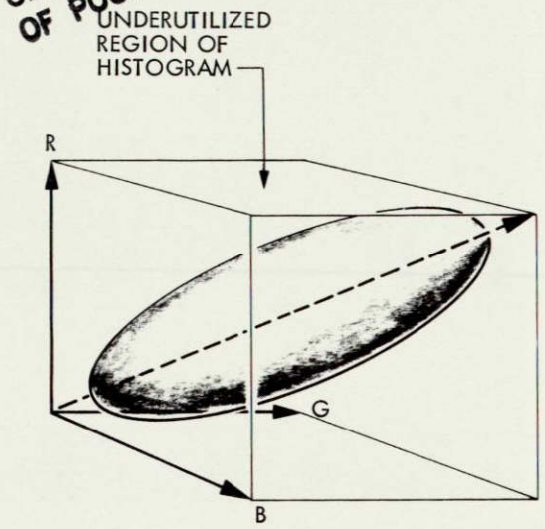

Figure 2.1(b) Contrast enhancement of individual components enlarges the distribution, but underutilized regions representing unused color range remain, since correlation is still present.

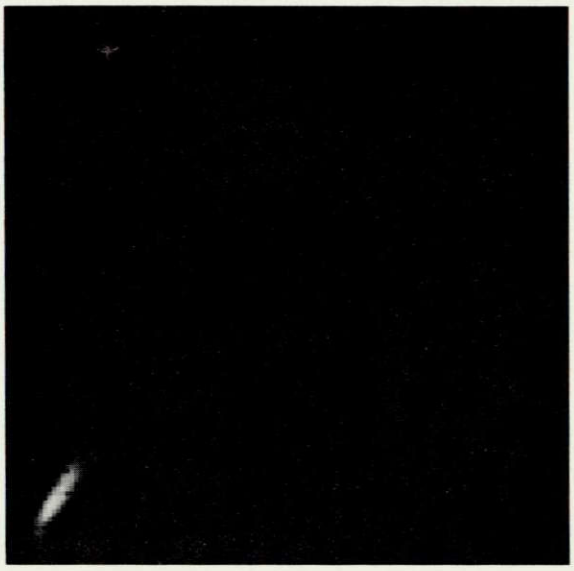

Figure 2.2(a) A 2-dimensional frequency of occurrence histogram (log population proportional to brightness) for MSS4 vs MSS5 of unprocessed LACIE segment 1739, acquisition 76282.

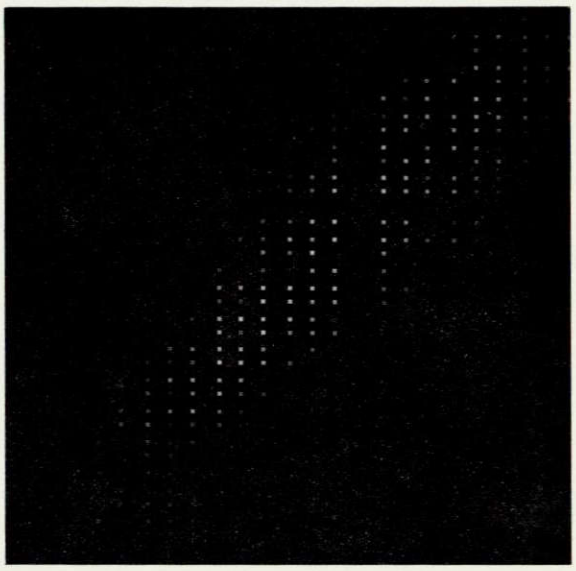

Figure 2.2(b) Similar histogram after processing to produce LACIE product 1.

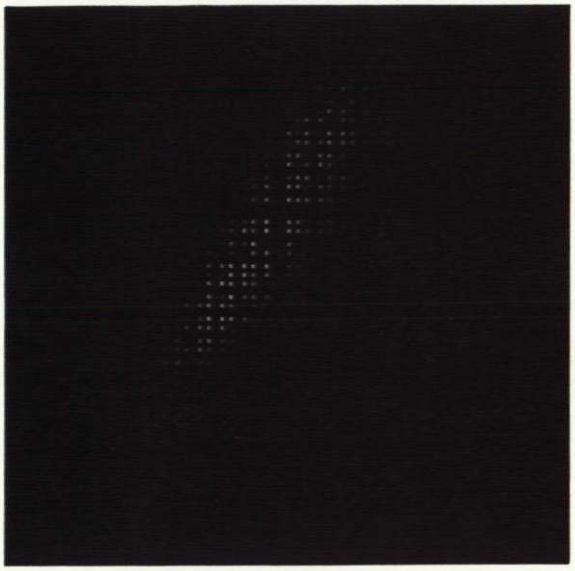

Figure 2.2(c) Regions of unused color are readily visible in histogram of LACIE product 3.

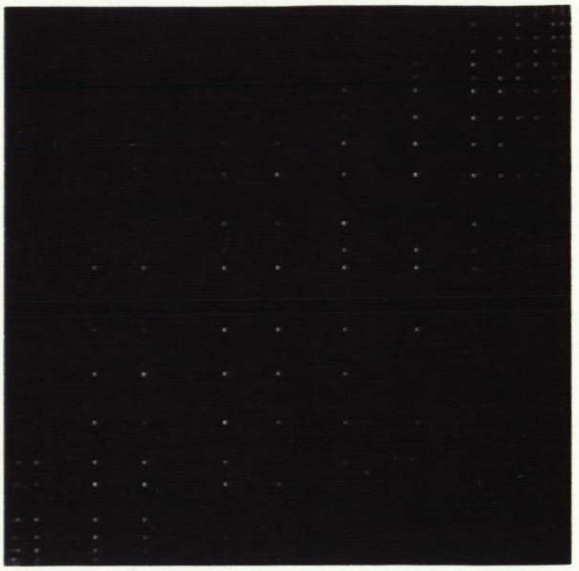

Figure 2.2(d) Correlation remains apparent even after the application of a non-linear contrast enhancement to individual components.

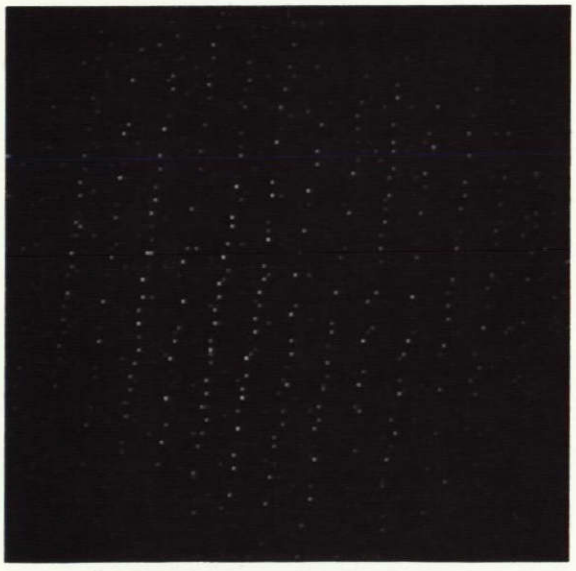

Figure 2.2(e) Decorrelation enhancement with linear variance equalization produces fuller utilization of color range.

Figure 2.2(f) Histogram after decorrelation enhancement with Gaussian variance equalization.

the principal component images are each contrast enhanced such that the resulting variances of the components are all equal, then any further rotation can be applied without introducing correlation (Ref. 1). Thus uncorrelated image components can be produced for any possible set of coordinate axes simply by performing a principal component transformation, contrast enhancing each component to equalize their variances, and then rotating to the desired coordinates. Assuming that the variance is appropriately chosen, a color composite display of components processed in this manner will include a wide range of color.

One coordinate system is preferable for the LACIE application, namely that system formed by the original image components. These coordinates can be reattained in the decorrelation procedure by following the variance equalization contrast enhancement by a rotation which is the inverse of the principal component rotation which was used. The primary reason for favoring this return rotation is that it allows the basic color relationships of the original scene to be preserved. Thus while absolute colors may sometimes be changed, an area that was redder than average, for example, in the original scene will remain redder than average after enhancement. This property can be particularly valuable to LACIE analysts, who are already attuned to the color relationships inherent in the current LACIE color products.

The contrast enhancement applied to the principal components to equalize their variance can be either linear or non-linear. Probably the most effective non-linear transformation is a mapping which forces the histogram of each principal component to be Gaussian (within quantization limitations). The resulting n-dimensional histogram will be a spherically symmetric Gaussian distribution (Ref. 2) as will any 3-dimensional subspace histogram. The relative advantages of either approach more or less parallel those for black and white image enhancement. The Gaussian approach forces a more balanced distribution of color, and hence is more likely to show differences existing in the input data. The linear technique on the other hand tends to preserve biases which exist in the input distribution. These biases (e.g., a predominance of one crop type) may be significant, and would be distorted by the Gaussian approach. To permit full evaluation of the decorrelation enhancement technique, both approaches were applied to the LACIE test data. The effectiveness of either technique in removing interband correlation is demonstrated in the 2-dimensional histograms of Figure 2.2.

information which is more absolute in meaning and less relative to average scene properties. Such an approach of course required that all scenes be normalized to remove the effects of all external variables, such as solar illumination angle, atmospheric path length, and atmospheric haze. In practice such normalization is difficult to perform since adequate information is not available. The results of our experiments with global transformations and scene normalization are described in Section 4.

Another significant consideration in applying the decorrelation enhancement procedure is the presence of noise. In the principal component transformation, total scene variance (summed over all components) is unchanged by the rotation (Ref. 5). Since scene information (variance) is concentrated into the higher order principal component(s), the lower order component(s) will naturally contain less variance than the original bands. Noise, on the other hand, should be uncorrelated and hence will remain equally distributed among the components after the principal component rotation. Table 2.2 illustrates the situation by listing approximate signal-to-noise ratios (SNRs) for the principal components in the 3-dimensional transformation applied to four acquisitions of segment 1739 (SNRs are given as ratios of standard deviations, not variances). An approximate value for noise variance in each case was obtained by assuming that the fourth component in a 4-dimensional principal component transformation is composed only of noise, which is not actually true. The relatively poorer signal to noise ratios of the lower order components, particularly for V3 (the third principal component) is apparent (the basically noisy character of Landsat data as seen by the low average signal to noise ratio of the original components, is also apparent). Now as the variance of all components is equalized in the decorrelation enhancement process, the noise level in the third component will be increased by a much greater margin than will the noise level of the first component (the applied gain is inversely proportional to the SNR). In fact it can be seen that the noise (and, of course, the signal) in both components 2 and 3 will be increased by a greater amount than would have been the case were the original channels enhanced individually (as in the case for LACIE products 1 and 3). The resulting higher noise level, due particularly to the strong gain applied to the third component, appears as color speckle in the enhanced product. The same effect was noted by Juday when he used Kauth components to enhance color (Ref. 4). Inspection of the third principal component reveals that there is meaningful low and intermediate frequency

data in the image. The approach used in this study to preserve the discriminating capability of this information while reducing the confusing influence of noise was to smooth the third, and sometimes the second, principal component by low pass filtering. While simple box filtering (averaging of nearby elements) was used in some cases, best results were obtained using a two dimensional low pass median filter (Ref. 6). This filter offers the capability of smoothing within a field while leaving the field boundary nearly intact. Details of the filtering procedures can be found in Section 4, and in Appendix 6.1. Before proceeding with a discussion of techniques and results, a summary of the products produced for this study will be presented.

3. DESCRIPTION OF PROCESSING TECHNIQUES

This section defines the various enhancement techniques used to process the imagery in this study. For identification purposes each technique was assigned a two digit product code (PRC) number. This number is found beneath each image following the letters PRC. Table 3.2 summarizes the 24 product types produced during the course of this study. Terms which are used in the product codes description of Table 3.2 are defined in Table 3.1.

Products 04-25 all utilize forward and reverse principal component transformations. Unless otherwise specified, the statistics used in generating a particular principal component transformation will have been obtained from the individual acquisition under consideration. The forward transformation generates principal components V_i. These components are then processed (filtered, enhanced to equalize variances, etc.) and the reverse transformation applied. This produces components B_i. As shown in Section 2, the reverse transformation domain coincides with the original input domain. The components B_i are then displayed as primary colors.

Table 3.3 summarizes the extent of the application of the various techniques to the working data set.

TABLE 3.1 Definition of Terms

FPCT	Forward principal component transformation
RPCT	Reverse principal component transformation
V1	1st principal component
V2	2nd principal component
V3	3rd principal component
V4	4th principal component
B1	1st reverse transformation component
B2	2nd reverse transformation component
B3	3rd reverse transformation component
B4	4th reverse transformation component
GVE	Gaussian variance equalization
LVE	Linear variance equalization
Rσ	The real number R followed by the letter σ describes the nature of the variance equalization method used. Its meaning is twofold: In the case of linear variance equalization (LVE), the real number R specifies the number of standard deviations on either side of the mean of the distribution that remain unsaturated after the linear contrast enhancement is performed to fix the variance. In the case of Gaussian variance equalization (GVE), the real number R specifies the extent of the reference Gaussian distribution. The distribution being processed is then matched to the truncated Gaussian distribution by matching cumulative distribution functions, hence fixing the variance.

TABLE 3.2 Product Codes Description

PRC	INPUT BANDS	PROCESSING DESCRIPTION
01	MSS 4,5,7	LACIE product 1
03	MSS 4,5,7	LACIE product 3
04	MSS 4,5,6,7	FPCT based on statistics for all acquisitions in the given segment. GVE 2.3σ of V1-V4. RPCT. B1=blue; B2=green; B4=red.
05	MSS 4,5,6,7	FPCT based on statistics for all acquisitions for the entire working data set. GVE 2.3σ of V1-V4. RPCT. B1=blue; B2=green; B4=red.
06	MSS 4,5,6,7	FPCT based on statistics for all acquisitions in the given segment. V3 low pass filtered with a 3x3 box of equal weights. V4 low pass filtered with a 7x7 box of equal weights. GVE 2.3σ of V1-V4. RPCT. B1=blue; B2=green; B4=red.
07	MSS 4,5,6,7	FPCT based on statistics for all acquisitions for the entire working data set. V3 low pass filtered with a 3x3 box of equal weights. V4 low pass filtered with a 7x7 box of equal weights. GVE 2.3σ of V1-V4. RPCT. B1=blue; B2=green; B4=red.
08	MSS 4,5,6,7	FPCT. V3 low pass filtered with a 3x3 box of equal weights. GVE 2.3σ of V1-V3. V4 was omitted in the reverse transformation. RPCT. B1=blue; B2=green; B4=red.
09	MSS 4,5,7	FPCT. V3 low pass filtered with a 3x3 box of equal weights. GVE 2.3σ of V1-V3. RPCT. B1=blue; B2=green; B3=red.
10	MSS 4,5,7	FPCT. V3 filtered with a 3x3 median filter (see Appendix 6.1) GVE 2.3σ RPCT. B1=blue; B2=green, B3=red.
11	MSS 4,5,7	FPCT. V3 filtered with a 5x5 median filter (see Appendix 6.1). GVE 2.3σ of V1-V3. RPCT. B1=blue; B2=green; B3=red.
12	MSS 4,5,7	FPCT. V3 filtered with a 3x3 mode filter (see Appendix 6.1). GVE 2.3σ of V1-V3. RPCT. B1=blue; B2=green; B3=red.
13	MSS 4,5,7	FPCT. V3 filtered with a 5x5 mode filter (see Appendix 6.1). GVE 2.3σ of V1-V3. RPCT. B1=blue; B2=green; B3=red.
14	MSS 4,5,7	FPCT. V3 low pass filtered with the following 3x3 box: 1 1 1 1 2 1 1 1 1

GVE 2.3σ of V1-V3. RPCT. B1=blue; B2=green; B3=red.

15 MSS 4,5,7 FPCT. V3 low pass filtered with the following 5x5 box:

```
1 1 1 1 1
1 2 2 2 1
1 2 2 2 1
1 2 2 2 1
1 1 1 1 1
```

GVE 2.3σ of V1-V3. RPCT. B1=blue; B2=green; B3=red.

16 MSS 4,5,7 FPCT. V3 low pass filtered with the following 5x5 box:

```
1 1 1 1 1
1 1 1 1 1
1 1 1 1 1
1 1 1 1 1
1 1 1 1 1
```

GVE 2.3σ of V1-V3. RPCT. B1=blue; B2=green; B3=red.

17 MSS 4,5,7 FPCT. V3 low pass filtered with the following 7x7 box:

```
1 1 1 1 1 1 1
1 2 2 2 2 2 1
1 2 3 3 3 2 1
1 2 3 4 3 2 1
1 2 3 3 3 2 1
1 2 2 2 2 2 1
1 1 1 1 1 1 1
```

GVE 2.3σ of V1-V3. RPCT. B1=blue; B2=green; B3=red.

18 MSS 4,5,7 FPCT. V3 low pass filtered with a 3x3 box of equal weights. LVE 2.0σ of V1-V3. RPCT. B1=blue; B2=green; B3=red.

19 MSS 4,5,7 FPCT. V2 filtered with a 3x3 median filter; V3 filtered with a 5x5 median filter (see Appendix 6.1). LVE 2.0σ of V1-V3. RPCT. B1=blue; B2=green; B3=red.

20 MSS 4,5,7 Input bands first adjusted for sunangle and atmospheric effects (see Appendix 6.2). FPCT based on statistics for all acquisitions in the given segment. V2 filtered with a 3x3 median filter; V3 filtered with a 5x5 median filter (see Appendix 6.1). GVE 2.3σ of V1-V3. RPCT. B1=blue; B2=green; B3=red.

21 MSS 4,5,7 Input bands first adjusted for sunangle and atmospheric effects (see Appendix 6.2). FPCT based on statistics for all acquisitions in the given segment. V2 filtered with a 3x3 median filter; V3 filtered with a 5x5 median filter (see Appendix 6.1). GVE 1.0σ of V1-V3. RPCT. B1=blue; B2=green; B3=red.

22	MSS 4,5,7	FPCT. GVE 2.3σ of V1-V3. RPCT. B1=blue; B2=green; B3=red.
23	MSS 4,5,7	FPCT. LVE 2.0σ of V1-V3. RPCT. B1=blue; B2=green; B3=red.
24	MSS 4,5,7	Input bands first multiplied by a binary mask to exclude non-agricultural regions. FPCT based on included regions only. GVE 2.3σ of V1-V3. RPCT. B1=blue; B2=green; B3=red.
25	MSS 4,5,7	Input bands first multiplied by a binary mask to exclude non-agricultural regions. FPCT based on included regions only. GVE 2.3σ of V1-V3. V2 and V3 filtered with a 3x3 median filter (see Appendix 6.1). RPCT. B1=blue; B2=green; B3=red.

TABLE 3.3 PROCESSING SUMMARY

SEGMENT NUMBER	Product Code (PRC)																							
	1	3	4	5	6	7	8	9	10	11	12	13	14	15	16	17	18	19	20	21	22	23	24	25
1000	X	X					X	X									X	X						
1183	X	X					X	X									X	X						
1531	X	X					X	X									X	X			X	X	X	X
1537	X	X					X	X									X	X						
1606	X	X					X	X									X	X						
1625	X	X	X	X	X	X	X	X									X	X						
1637	X	X	X	X	X	X	X	X									X	X			X	X	X	X
1648	X	X					X	X									X	X						
1734	X	X					X	X	X	X	X	X	X	X	X	X	X	X	X	X				
1739	X	X					X	X									X	X	X	X				
9930	X	X					X	X									X	X						
9931	X	X					X	X									X	X						

4. DISCUSSION AND EVALUATION

The purpose of this section is to provide a preliminary evaluation of the various processing techniques utilized in this study. The intent here is to make observations based on the IPL's experience in multispectral image enhancement. Final analysis and evaluation will rest with JSC personnel.

As a first step, IPL equivalents of LACIE products 1 and 3 (Ref. 7 Section 2) were created for all acquisitions of the working data set. These were designated as products 01 and 03 respectively and were intended to provide a direct comparison for subsequent products generated at the IPL. The generation of products 01 and 03 also eliminated the problem of attempting to compare products generated at the IPL with those generated at JSC. All imagery was displayed as positive prints rather than positive transparencies in order to facilitate the comparison of large numbers of images without requiring the use of a light table.

Figures 4.1 and 4.2 display products 01 and 03 for four acquisitions of segment 1531. The 10 x 10 pixel grid was superimposed on all products generated in this study so as to reference the pixel to the upper left of a given grid intersection in a manner consistent with the standard LACIE grid system (Ref. 7 p. 4.6) Consequently, the pixels immediately to the upper right, lower right, and lower left of the grid intersection are partially overwritten by the grid lines in order to display the referenced pixel in its entirety.

As stated in Section 3, processing techniques 04-25 all utilize the decorrelation enhancement technique, employing forward and reverse principal component transformations. In Section 2, it was shown that the process of variance equalization in the principal component domain tends to accentuate the inherent uncorrelated noise in the data producing a color speckle in the end product. Since the solution of this problem is basic to the success of the method, the noise issue will be discussed first.

Products 22 and 23 were created solely to demonstrate the accentuation of color speckle as a result of the principal component transformation color enhancement technique. To illustrate the problem, figure 4.3 displays product 23 for the same acquisitions of segment 1531 as above. Product 22 possessed virtually the same noise characteristics as product 23 and will not be included here. While there is obviously more color in product 23 as compared to products 01 and 03, there is also substantially more color speckle. The problem was to develop

techniques which preserve the feature color boundaries (e.g., field boundaries) and at the same time, suppress the extraneous color speckle.

As shown in Section 2, the signal to noise ratio decreases dramatically in the lower order principal components. For this reason, the speckle problem was attacked by performing noise reduction operations in the principal component domain before transforming back to the original input domain. In this study, various filters were applied to the lower order principal components in an effort to suppress the color speckle in the end products.

Figure 4.4 displays product 18 for the same acquisitions as above. In this product, the third principal component was filtered with a 3x3 low pass box filter before the reverse transformation was applied. When compared to the corresponding product 23, it is apparent that the color speckle has been noticeably reduced. The next experiment then was to try different types of filters on the third principal component. In order to evaluate the extent of any field boundary degradation, acquisitions from segment 1734 were chosen to be the subject of this processing because of the multitude of well defined field boundaries. A total of eight different filters (see Section 3) was applied to the third principal component before the reverse transformation was performed, creating products 10-17. There were no readily visible differences in noise content between any of these products and the corresponding product 18, so the imagery is not included here. All of these products are included in the photoproducts supplement.

Inspection of the individual principal components for product 23 for segment 1531 revealed that the second principal component in some of the acquisitions possessed noticeable speckle. At this point, interest arose over the prospect of filtering two of the three principal components. Such a procedure would reduce the color speckle, but it might also blur the edge features in the process. However, the two dimensional median filter (See Appendix 6.1) used in products 10 and 11 has the property of preserving edge features and, at the same time, suppressing speckle noise. This gave rise to product 19, wherein the third principal component was filtered with a 5x5 median filter and the second principal component was filtered with a 3x3 median filter prior to the reverse transformation. Figure 4.5 exhibits product 19 for the same acquisitions displayed previously. There is a noticeable improvement over product 18, and upon close inspection, the color speckle noise level can be favorably compared with the corresponding product 01, while at the same time, the color range is dramatically

increased. In addition, the feature boundaries have been preserved. These results appeared to be favorable, so products 18 and 19 were made for all acquisitions of the working data set, and are included for evaluation in the supplemental photoproducts volume.

A given product was often intended to serve as a basis for evaluation of more than one processing technique. For example, products 18 and 19 were also created to evaluate the effects on color content of linear variance equalization as opposed to the Gaussian variance equalization employed in other products. With this in mind, the next topic for discussion is the nature of the color content produced by the various decorrelation techniques investigated in this study.

Figures 4.6 and 4.7 display products 01 and 03 for four acquisitions of segment 1606. Figures 4.8 and 4.9 display the corresponding products 08 and 09 for the same acquisitions. Chronologically, products 08 and 09 were the first color products created at the IPL by generating the principal component statistics using the individual acquisition under consideration. In order to evaluate the general promise of the technique, products 08 and 09 were made for all acquisitions of the working data set. The results show a dramatic increase in the color range, as can be seen by comparing figures 4.6 - 4.9. Aside from a first pass at acquisition specific color enhancement, products 08 and 09 also provide a comparison between the input of MSS 4, 5, 6, and 7, and the input of MSS 4, 5, and 7 into the principal component transformation. Even though it is well known that there is a very high degree of correlation between MSS 6 and MSS 7, it remained to be seen if the addition of MSS 6 to MSS 4, 5, and 7 in the decorrelation enhancement process would yield additional information in the color end product. Gaussian variance equalization of the principal components was employed in both products, matching distribution functions (histograms) to a truncated Gaussian distribution of $\pm 2.3\sigma$. There appear to be no significant differences in color information between these two products, as shown in figures 4.8 and 4.9. Since processing four input bands instead of three obviously requires more time, subsequent products were generated from MSS 4, 5, and 7 only.

Next, the choice of the variance equalization method used in the principal component domain will be discussed. As pointed out in Section 2, the nature of the Gaussian variance equalization method can alter signal relationships in the principal component domain in a non-linear fashion. This can affect both the

noise and the color characteristics of the end products. To evaluate the relative merits of the two variance equalization methods, product 18 was created for a direct comparison to product 09. Product 09 employs Gaussian variance equalization while product 18 employs linear variance equalization: Figure 4.10 displays the corresponding product 18 for the same acquisitions of segment 1606 as above. In this example, there appears to be more color definition in the product 18 version. In particular, the diagonal feature running through the lower left portion of the image seems to be more distinctly separable from its immediate surroundings in product 18 than in product 09. It is important to note however that if the initial distributions of the principal components closely resemble Gaussian distributions, then the two variance equalization methods used in products 09 and 18 will yield very similar results. This effect can be seen in figures 4.14 and 4.15. Since product 19 showed reasonable promise as discussed previously, its results for the segment 1606 acquisitions are also included here, in figure 4.11, to afford the reader another opportunity to evaluate the effects of the two dimensional median filters applied to the principal components. Prints of products 18 and 19 for the entire test data base are included in the supplement.

The next issue to be addressed is the color consistency between acquisitions for the various products using the principal component transformation. An examination of figures 4.6 to 4.11 shows that the various colors present in products 01 and 03 generally remain readily identifiable in products 08, 09, 18, and 19 but in a very accentuated form. That is, a given color will retain its basic character and not be transformed to an entirely different color. Slight color shifts may occur, usually involving unsaturated colors in the products 01 and 03. However, basic color relationships are preserved in the enhancement process, so that enhanced colors possess a clear interpretive compatibility with current LACIE products. Color trends visible in a sequence of acquisitions in products 01 and 03 are also readily apparent after decorrelation enhancement. This basic color compatibility with current LACIE products, including similarity of variation across acquisitions, was a key design goal in the implementation of the enhancement process, and can be verified for the entire test data set by inspection of the photoproducts supplement.

Up to this point, all products discussed have been processed using acquisition specific statistics, as is the case with standard LACIE products. As shown above, the products utilizing some form of the decorrelation enhancement process

possess a greater color range than the corresponding products 01 and 03. For this reason, processing techniques were investigated which utilize the increased color range to maintain strict color consistency over an arbitrary selection of acquisitions. By strict color consistency, it is meant that a given input n-tuple of pixel values will produce the identical color in the end product, regardless of the acquisition in which it is found. To accomplish this, for each of the input bands (e.g., MSS 4, 5, and 7), a merged data set was created which contained the data for that band from all the acquisitions under consideration. The principal component transformation and the corresponding variance equalization parameters were generated using the statistics from the merged data sets. Each individual acquisition could then be processed using a fixed principal component transformation and variance equalization parameters, ensuring that the resulting color in the end products was consistent in all the acquisitions. Consequently, the color expansion was not optimal for any of the individual acquisitions but rather represented optimal processing for all the acquisitions taken together. Applying this process to the original test data produced product 04 which utilized statistics generated from all acquisitions in a given segment, and product 05 which utilized statistics generated from all the acquisitions in the entire working data set. Products 06 and 07 are filtered versions of products 04 and 05 respectively and do not differ in color content from them.

Not surprisingly, inadequate results were obtained when composite statistics gathered from sets of unnormalized input images were used. The individual acquisition data clusters in histogram space are somewhat segregated within the composite histogram, so that the color contrast in products 04 and 05 is low for all the individual acquisitions. The problem arises from the fact that variations in the acquisitions can be due both to real changes in the scene and to external influences which do not pertain to crop status. While the procedure aims to preserve the first category of variations, the second category is a significant noise factor which can introduce severe errors in interpreting real change. Thus ideally, all external influences would first be removed by normalizing the input scenes to "standard" viewing conditions.

Two external influences, namely variations in solar illumination angle and in atmospheric path length, can be easily modelled and removed. A detailed description of how this normalization was performed is given in Appendix 6.2. To obtain a color consistent decorrelation enhancement, then, individual acquisitions

are normalized before composite statistics are accumulated. Products 20 and 21 represent the results of this technique as applied to the generation of a segment specific principal component transformation and variance equalization parameters. Note that these two products differ only in the extent of the reference Gaussian distribution used in the variance equalization ($\pm 2.3\sigma$ for product 20 and $\pm 1.0\sigma$ for product 21). In addition, both products 20 and 21 employ two dimensional median filters in the principal component domain. To compare the end results, Figures 4.12 - 4.15 display products 01, 03, 09, and 19 for a sequence of four of the six acquisitions for segment 1739. Figures 4.16 and 4.17 display the corresponding products 20 and 21. Comparison of products 20 and 21 with products 01 03, 09, and 19 reveals a noticeable increase in the color range over products 01 and 03 but, as was expected, not as much of an increase as with products 09 and 19. There does seem to be slightly better contrast in product 21 than in product 20. This can be attributed to the more uniform distributions obtained as a result of the variance equalization utilizing a $\pm 1.0\sigma$ truncated Gaussian distribution instead of one of $\pm 2.3\sigma$. One would expect greater color speckle to accompany a harsher variance equalization. It appears however, as though the two dimensional median filters have successfully suppressed the speckle while retaining the slight increase in basic color differences. Finally, as a result of enforcing color consistency in products 20 and 21, the red color of the strip fields appears to increase in intensity as the growing season progresses. In products 01, 03, 09, and 19, the color of the strip fields remains basically the same. Products 20 and 21 then, may for this segment, more accurately reflect the crop maturation process. The degree to which the composite distribution (in histogram space) is tightened, relative to the distributions of individual acquisitions, provides a tool for assessing the impact of normalization. Details of the assessment procedure, together with results for several test segments, are provided in Appendix 6.3. Unfortunately, this processing technique did not yield results which were uniformly as promising as those shown here when applied to other segments. One significant external variable, atmospheric haze, was not removed, since its degree of influence is in practice not easily determined. The remaining variation among acquisitions is probably due to some combination of legitimate changes in scene spectral response and variations in atmospheric conditions, with possibly some other unidentified variables present. The normalization procedure does appear to be helpful in some cases. Further study might suggest heuristic procedures, for

example based on MSS4 mean value, which would allow haze effects to be adequately reduced.

Near the end of this study, products 24 and 25 were created in order to evaluate the effect of generating the principal component transformation based on the agricultural regions only. The intent was to attempt to force more color into regions of particular interest. This was done by first constructing a binary mask of a given segment using available ground truth. This mask contained a 1 where there was agriculture and a 0 everywhere else. Each band image of an acquisition within the segment was then multiplied by the mask image, leaving agricultural regions undisturbed and mapping non-agricultural regions to 0. The principal component transformation color enhancement technique was then applied to these images. For reasons which are as yet not fully understood, the color expansion was no more pronounced than with other products utilizing the principal component transformation based in the complete image. Since the masking process required forehand knowledge of the ground utilization, the technique was not studied further and the images created will not be shown here.

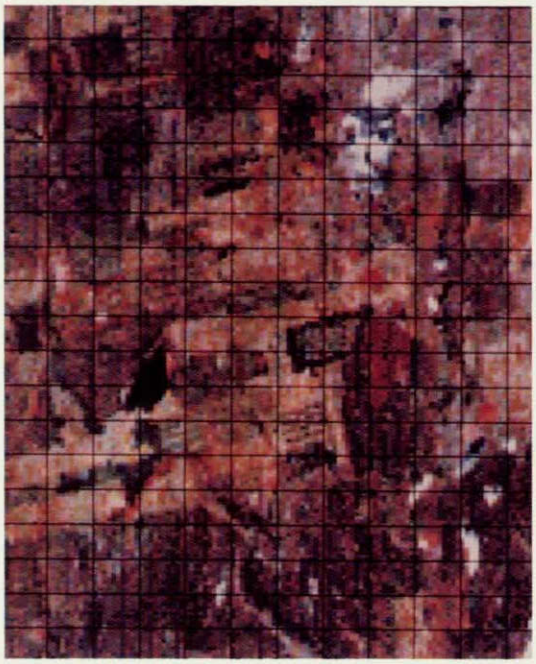

(b) Segment 1531 Acquisition 76315 PRC 01

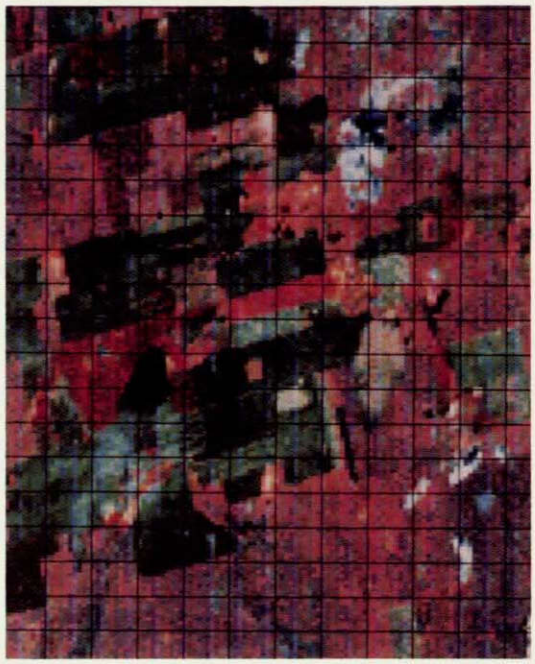

(d) Segment 1531 Acquisition 77129 PRC 01

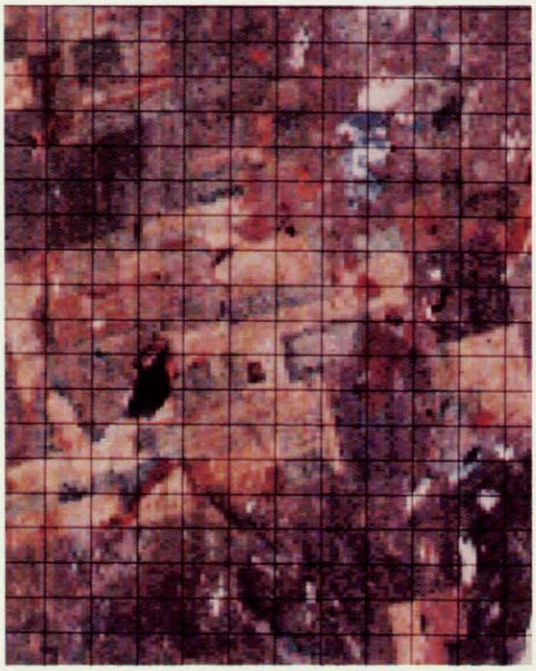

(a) Segment 1531 Acquisition 76279 PRC 01

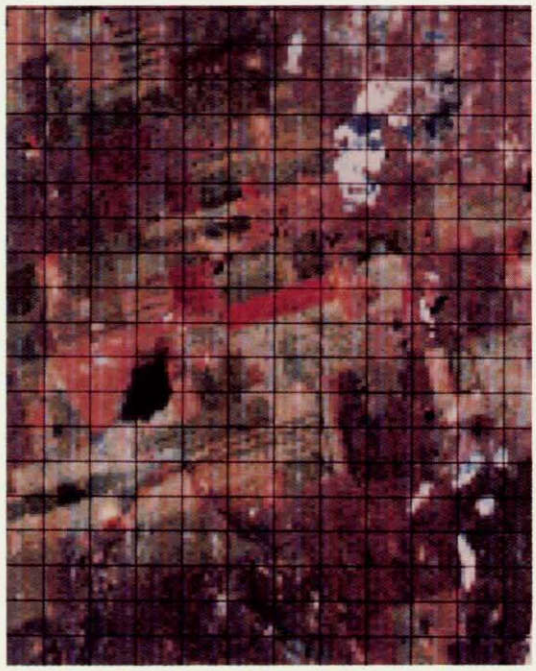

(c) Segment 1531 Acquisition 77112 PRC 01

Figure 4.1

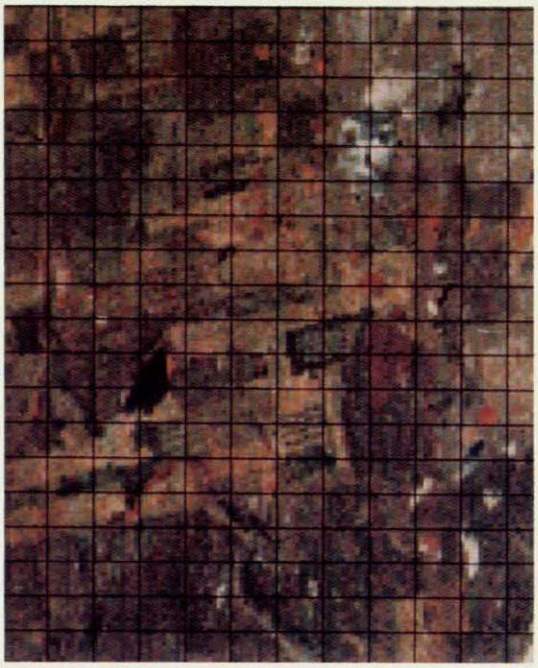

(b) Segment 1531 Acquisition 76315 PRC 03

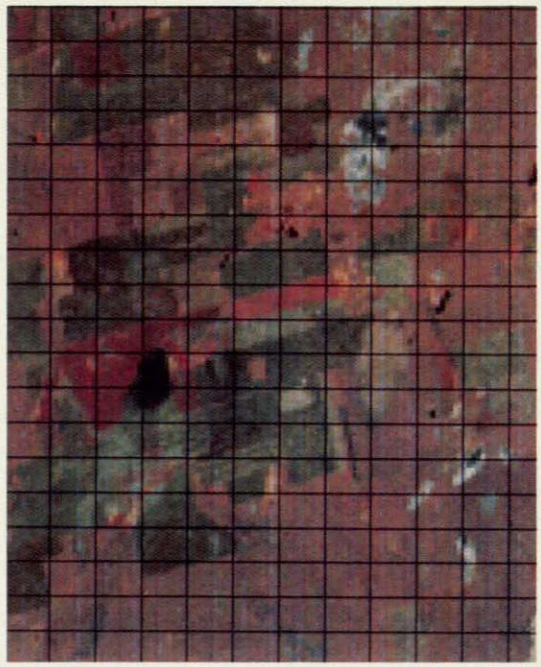

(d) Segment 1531 Acquisition 77129 PRC 03

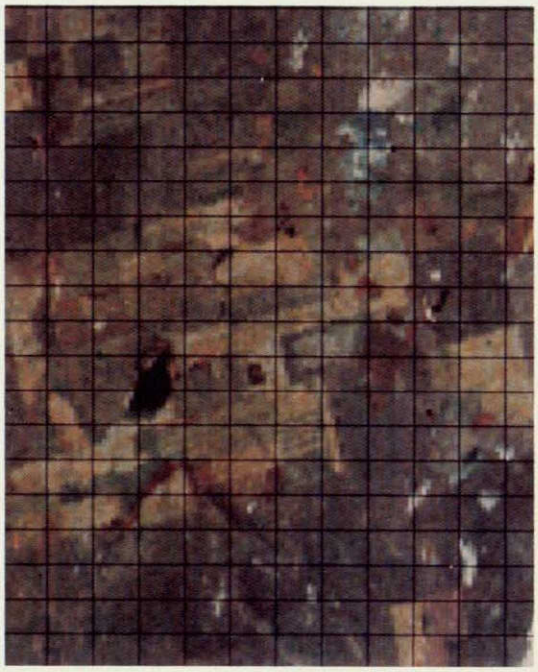

(a) Segment 1531 Acquisition 76279 PRC 03

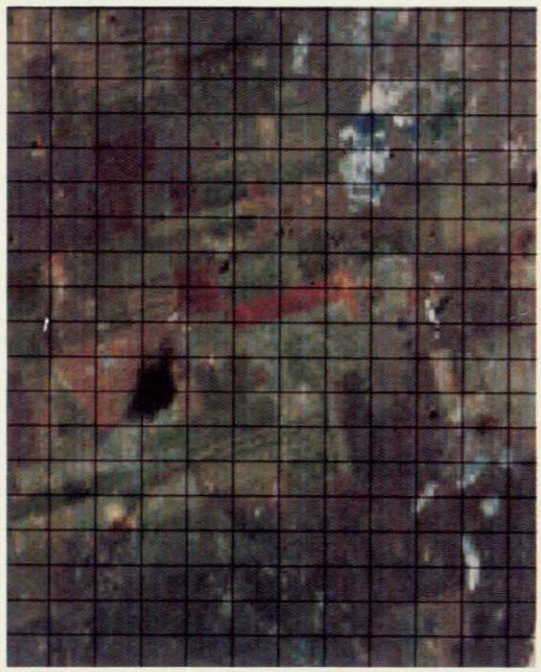

(c) Segment 1531 Acquisition 77112 PRC 03

Figure 4.2

(b) Segment 1531 Acquisition 76315 PRC 23

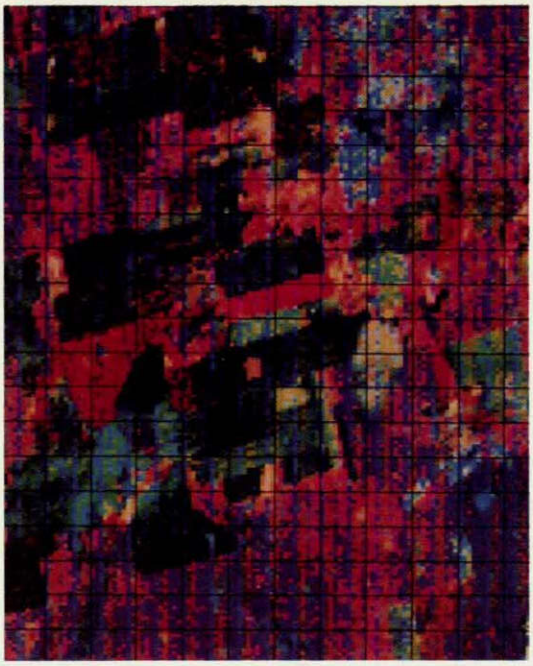

(d) Segment 1531 Acquisition 77129 PRC 23

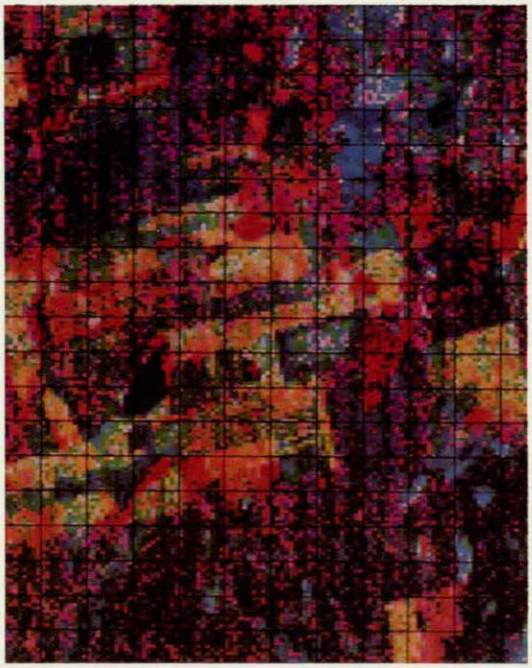

(a) Segment 1531 Acquisition 76279 PRC 23

(c) Segment 1531 Acquisition 77112 PRC 23

Figure 4.3

(b) Segment 1531 Acquisition 76315 PRC 18

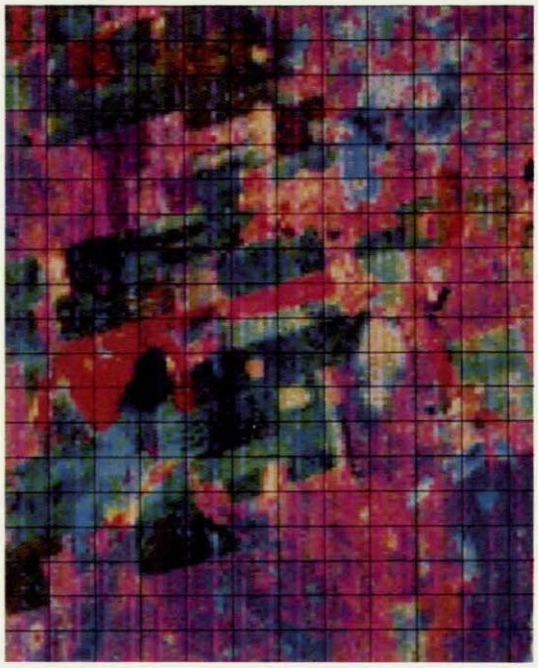

(d) Segment 1531 Acquisition 77129 PRC 18

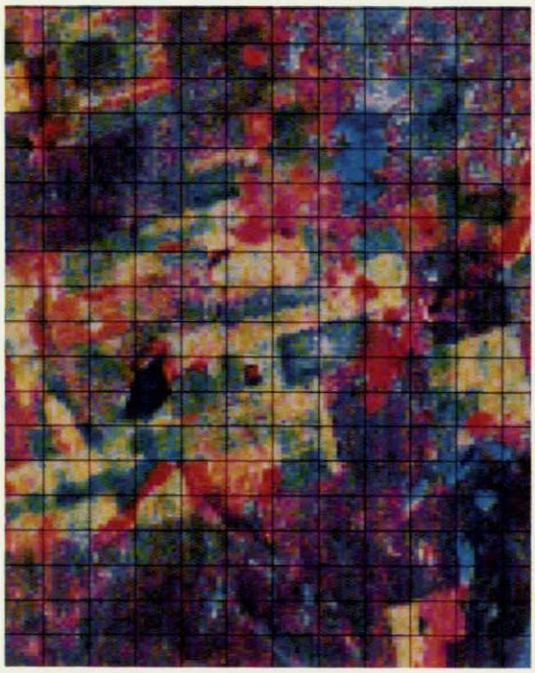

(a) Segment 1531 Acquisition 76279 PRC 18

(c) Segment 1531 Acquisition 77112 PRC 18

Figure 4.4

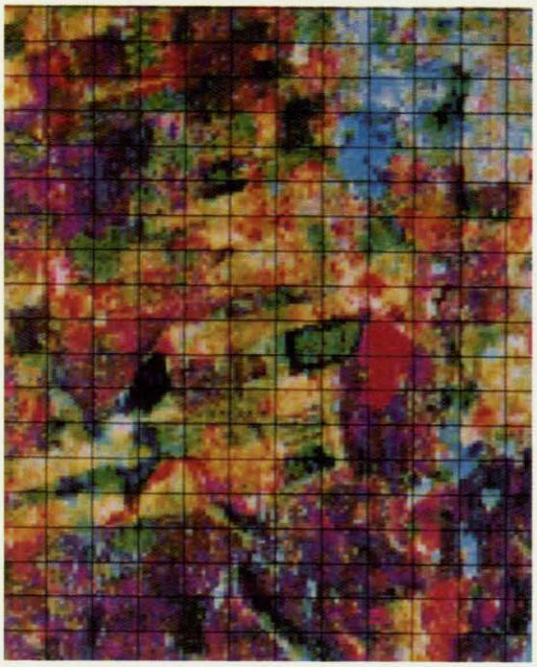

(b) Segment 1531 Acquisition 76315 PRC 19

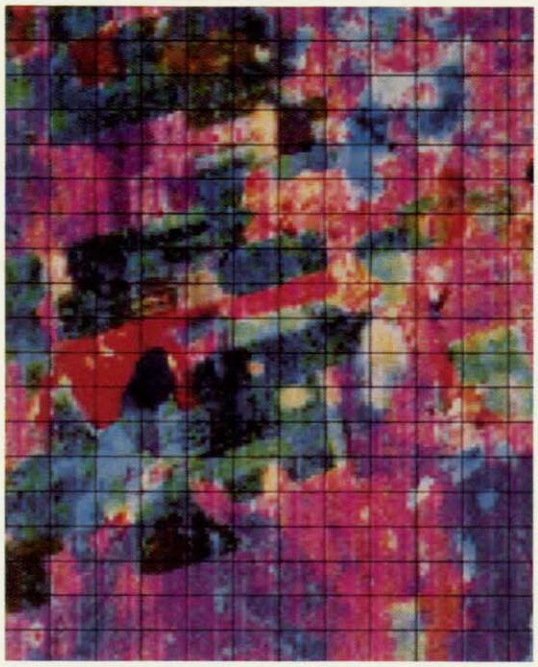

(d) Segment 1531 Acquisition 77129 PRC 19

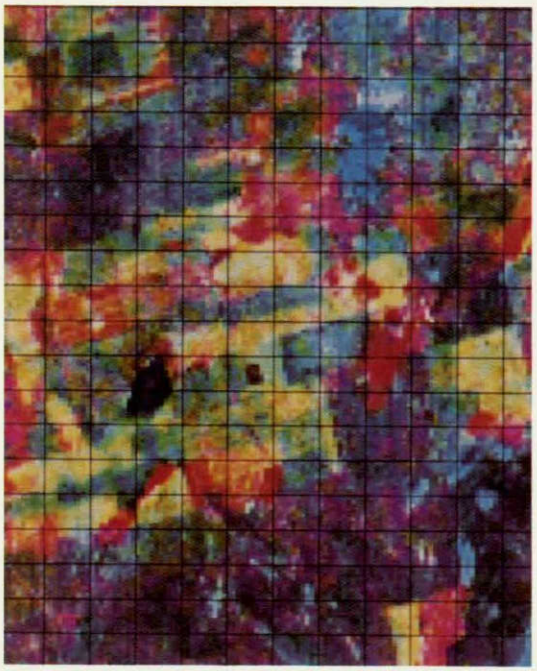

(a) Segment 1531 Acquisition 76279 PRC 19

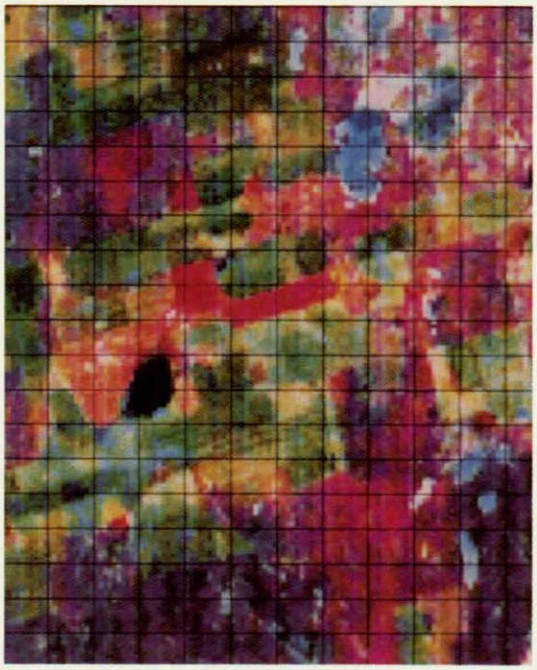

(c) Segment 1531 Acquisition 77112 PRC 19

Figure 4.5

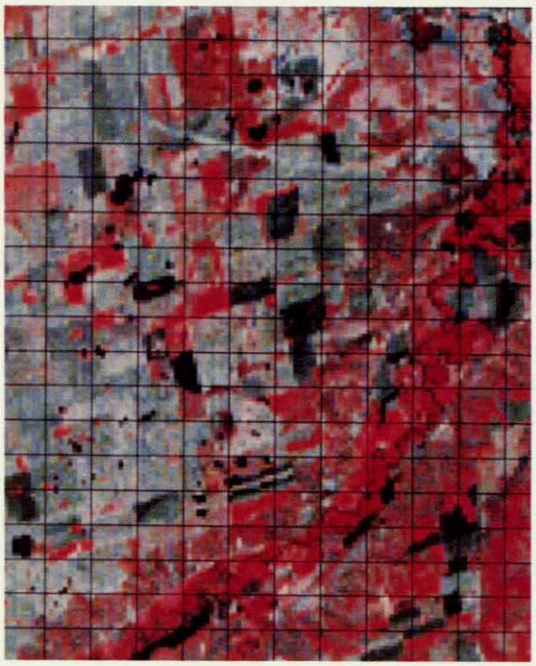

(b) Segment 1606 Acquisition 77143 PRC 01

(d) Segment 1606 Acquisition 77250 PRC 01

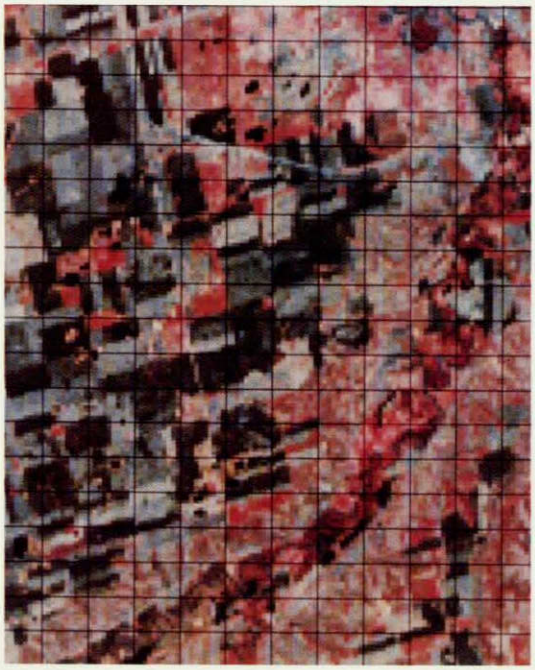

(a) Segment 1606 Acquisition 77125 PRC 01

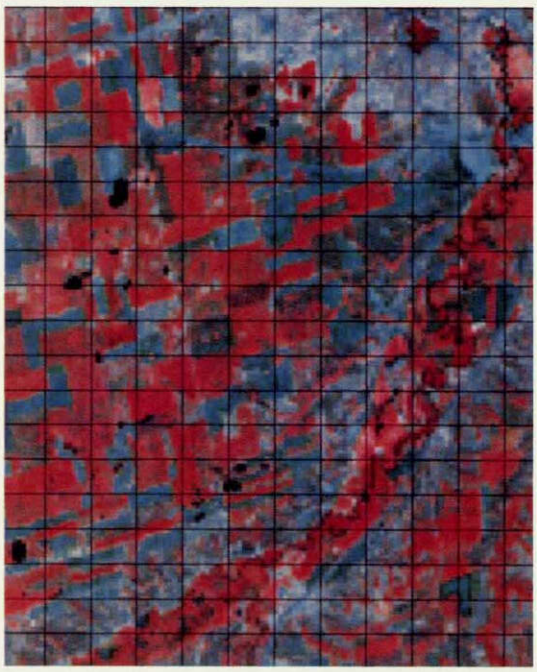

(c) Segment 1606 Acquisition 77197 PRC 01

Figure 4.6

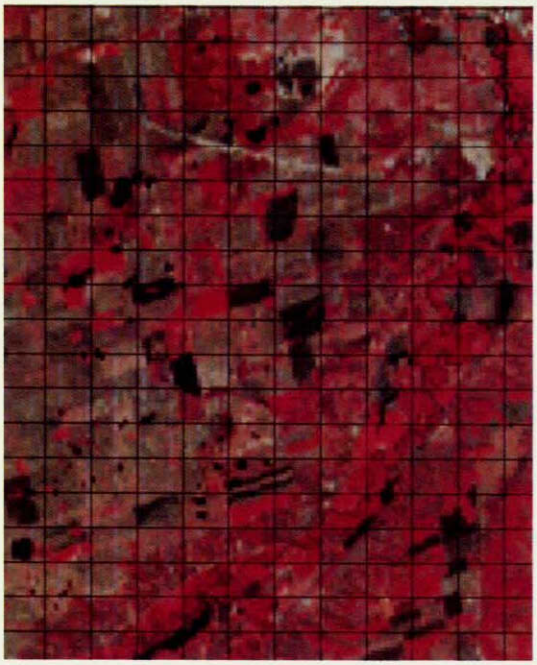

(b) Segment 1606 Acquisition 77143 PRC 03

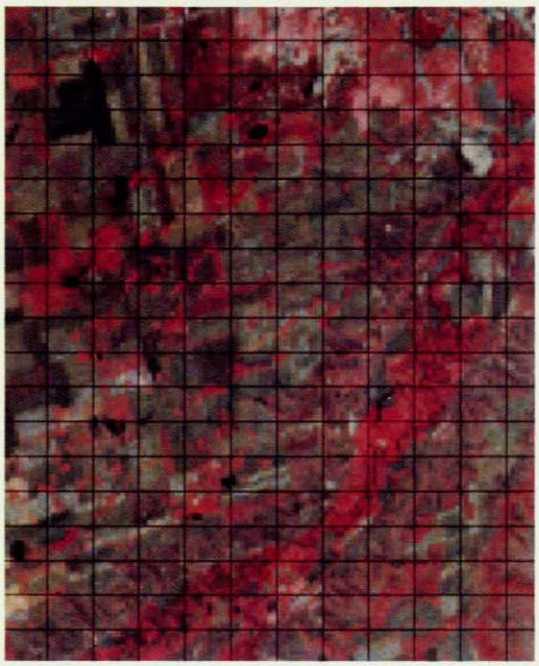

(d) Segment 1606 Acquisition 77250 PRC 03

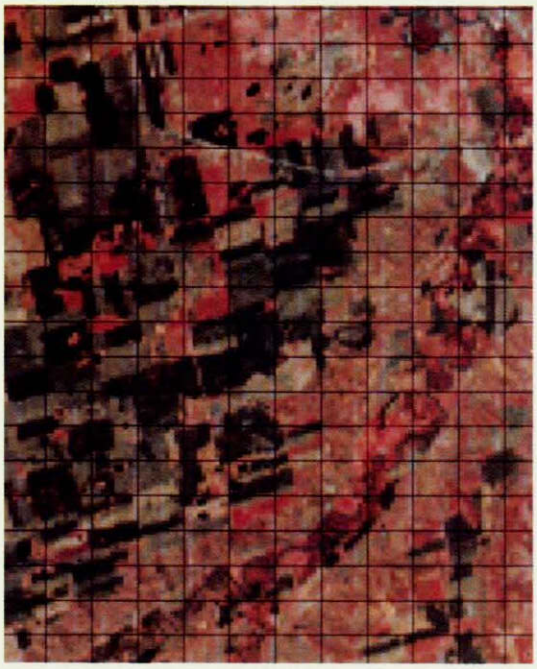

(a) Segment 1606 Acquisition 77125 PRC 03

(c) Segment 1606 Acquisition 77197 PRC 03

Figure 4.7

(b) Segment 1606 Acquisition 77143 PRC 08

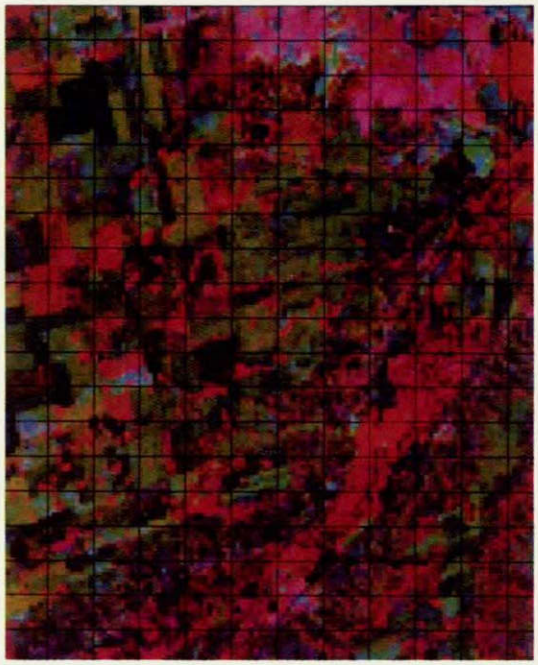

(d) Segment 1606 Acquisition 77250 PRC 08

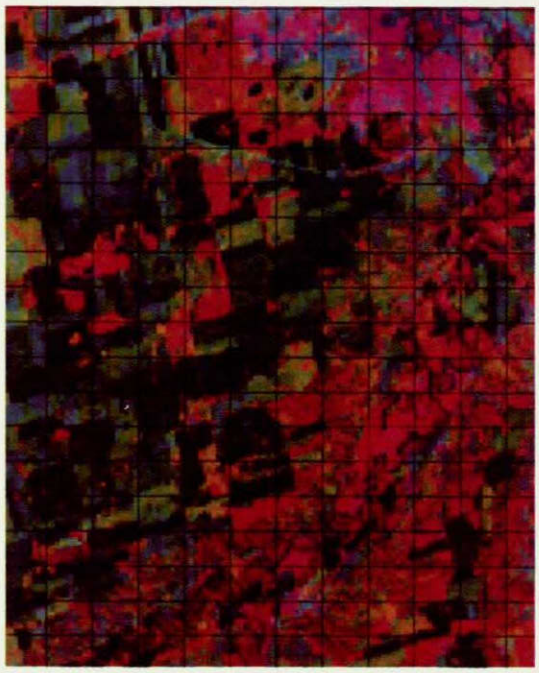

(a) Segment 1606 Acquisition 77125 PRC 08

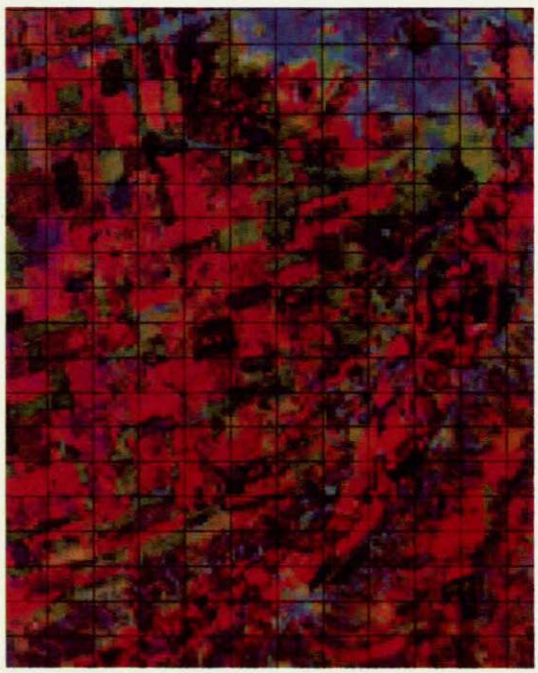

(c) Segment 1606 Acquisition 77197 PRC 08

Figure 4.8

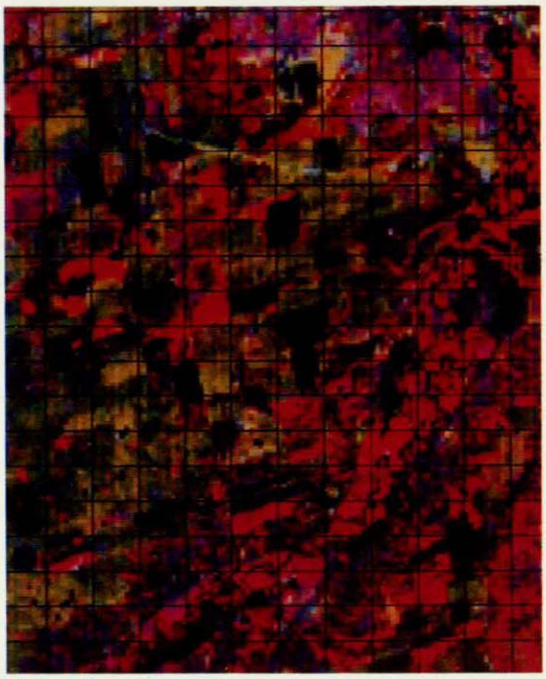

(b) Segment 1606 Acquisition 77143 PRC 09

(d) Segment 1606 Acquisition 77250 PRC 09

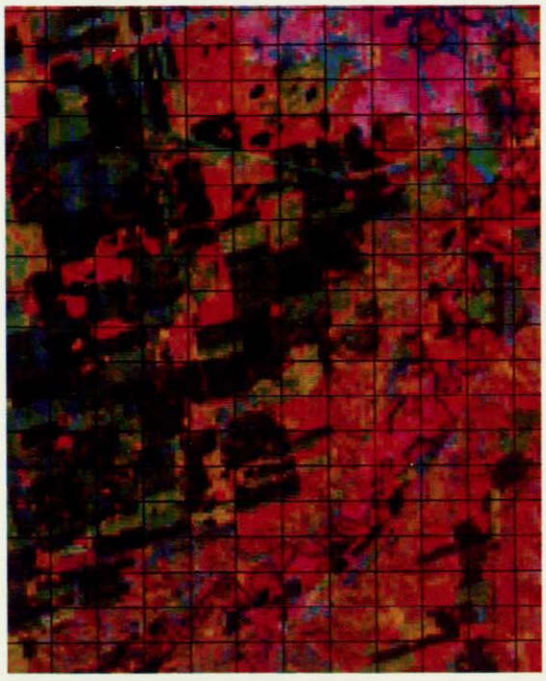

(a) Segment 1606 Acquisition 77125 PRC 09

(c) Segment 1606 Acquisition 77197 PRC 09

Figure 4.9

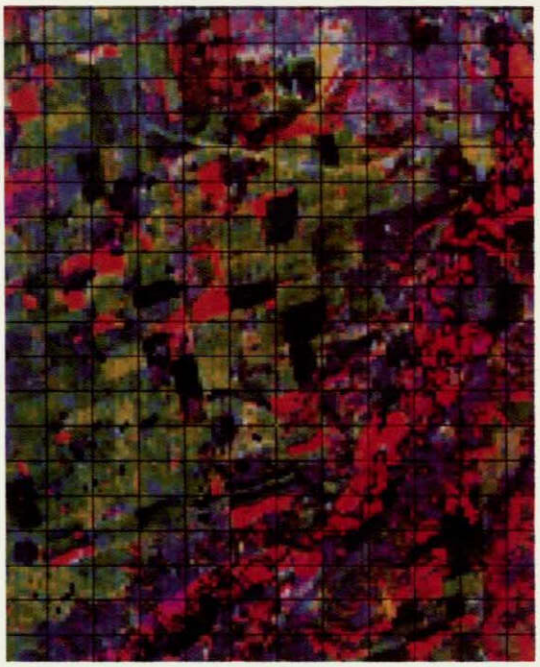

(b) Segment 1606 Acquisition 77143 PRC 18

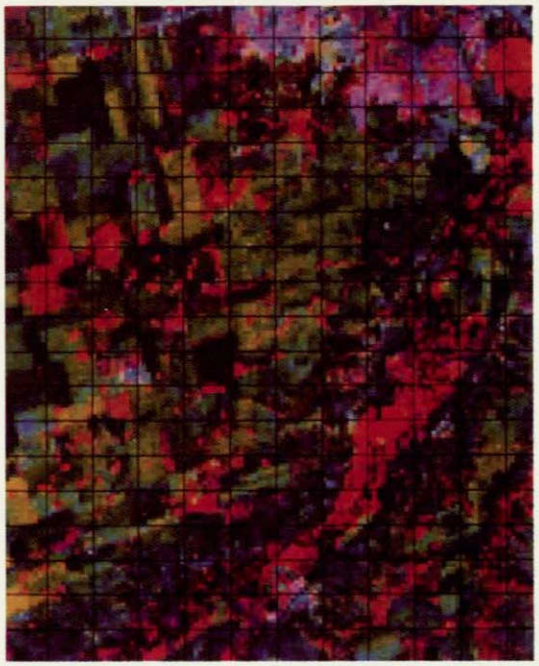

(d) Segment 1606 Acquisition 77250 PRC 18

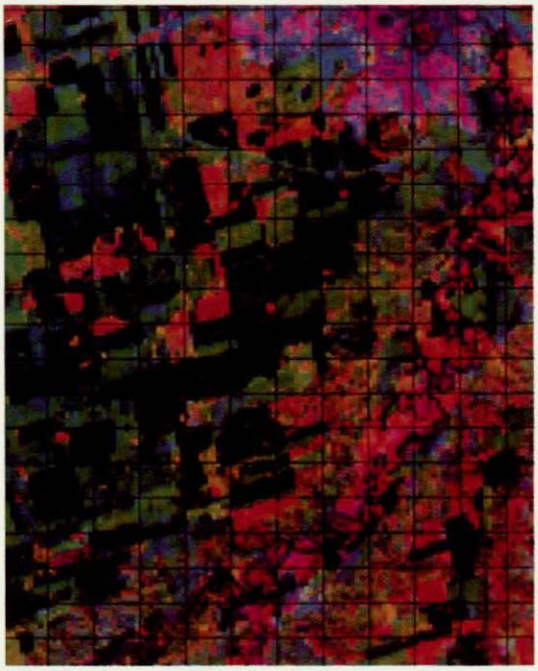

(a) Segment 1606 Acquisition 77125 PRC 18

(c) Segment 1606 Acquisition 77197 PRC 18

Figure 4.10

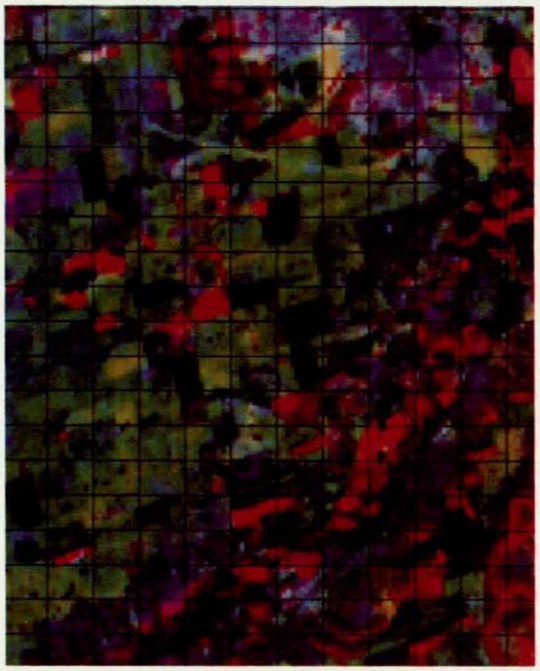

(b) Segment 1606 Acquisition 77143 PRC 19

(d) Segment 1606 Acquisition 77250 PRC 19

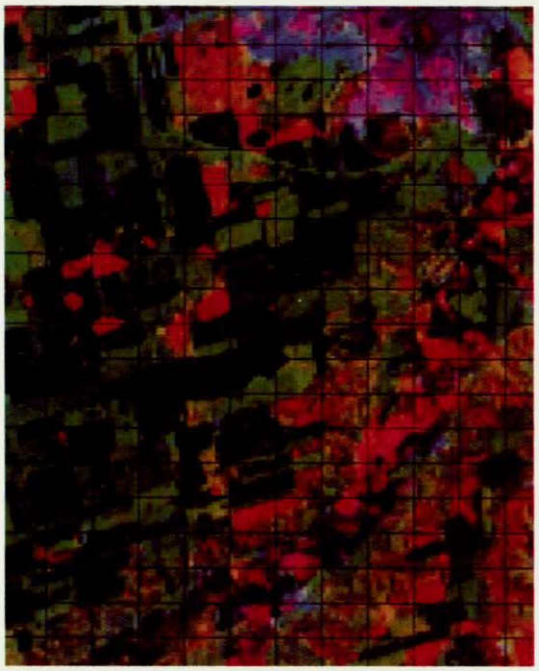

(a) Segment 1606 Acquisition 77125 PRC 19

(c) Segment 1606 Acquisition 77197 PRC 19

Figure 4.11

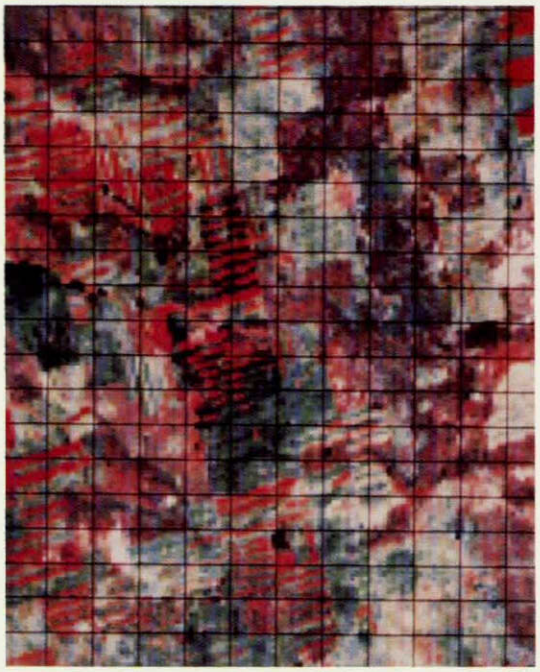

(b) Segment 1739 Acquisition 77132 PRC 01

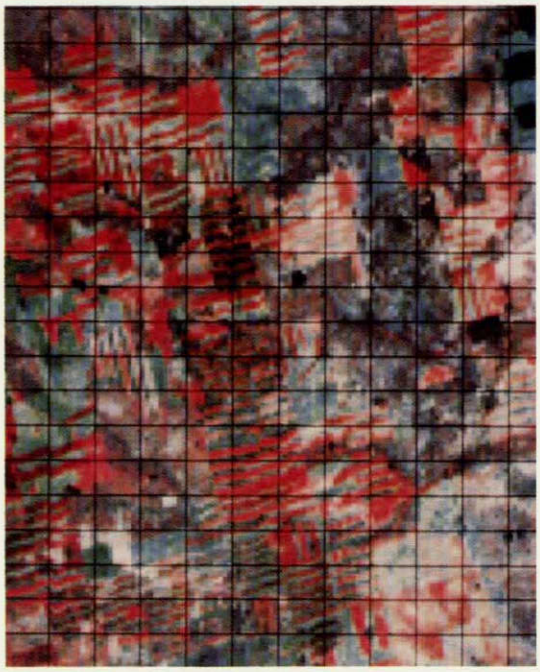

(d) Segment 1739 Acquisition 77168 PRC 01

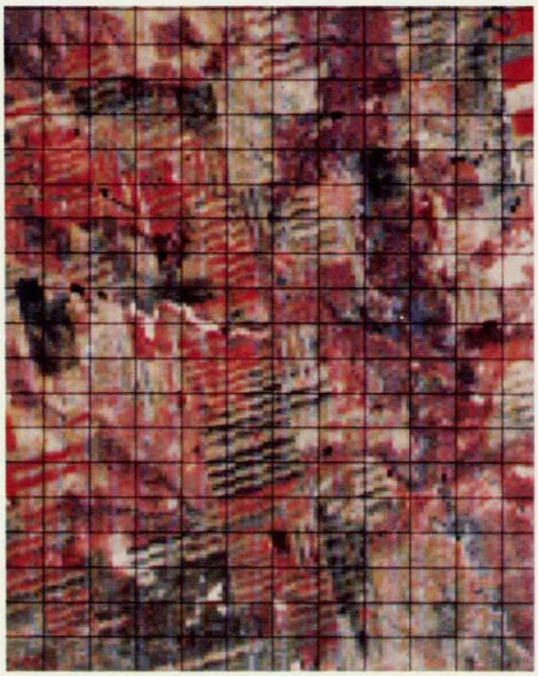

(a) Segment 1739 Acquisition 77114 PRC 01

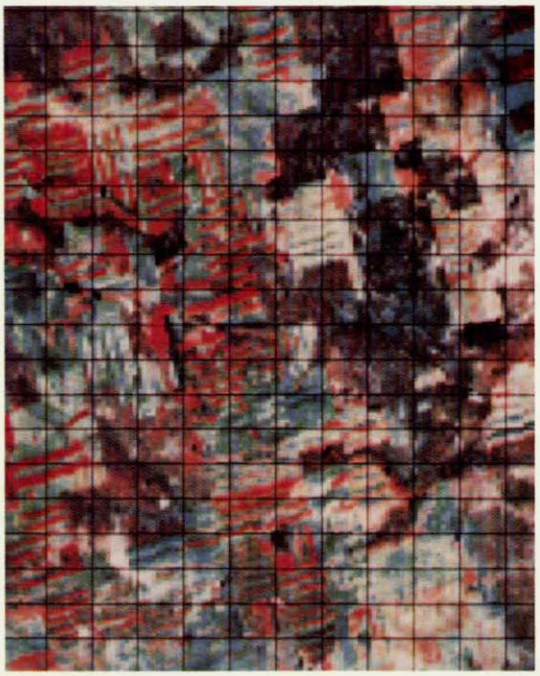

(c) Segment 1739 Acquisition 77150 PRC 01

Figure 4.12

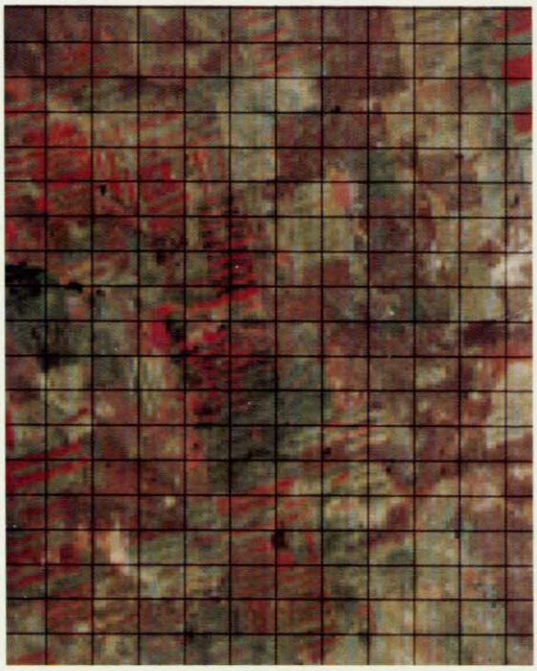

(b) Segment 1739 Acquisition 77132 PRC 03

(d) Segment 1739 Acquisition 77168 PRC 03

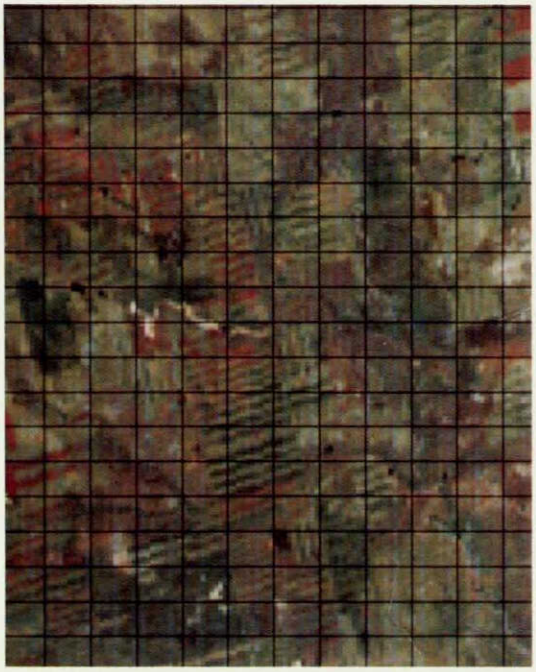

(a) Segment 1739 Acquisition 77114 PRC 03

(c) Segment 1739 Acquisition 77150 PRC 03

Figure 4.13

(b) Segment 1739 Acquisition 77132 PRC 09

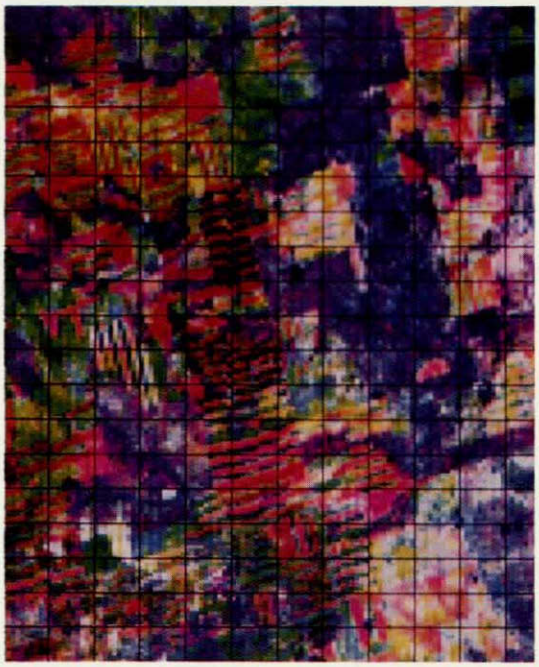

(d) Segment 1739 Acquisition 77168 PRC 09

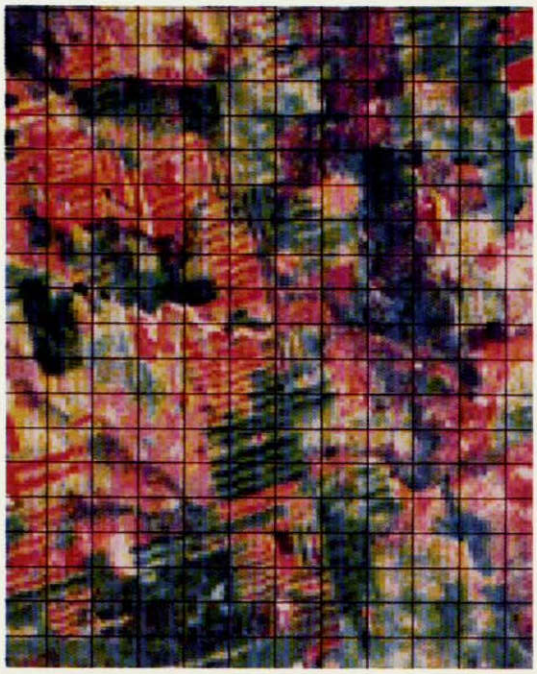

(a) Segment 1739 Acquisition 77114 PRC 09

(c) Segment 1739 Acquisition 77150 PRC 09

Figure 4.14

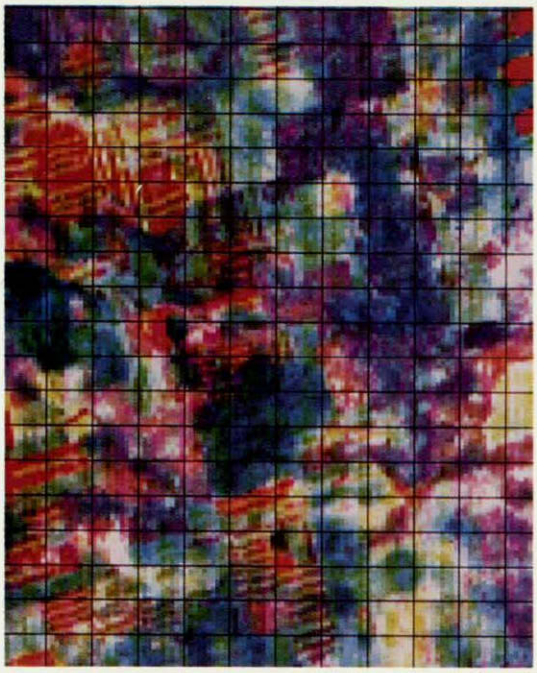

(b) Segment 1739 Acquisition 77132 PRC 19

(d) Segment 1739 Acquisition 77168 PRC 19

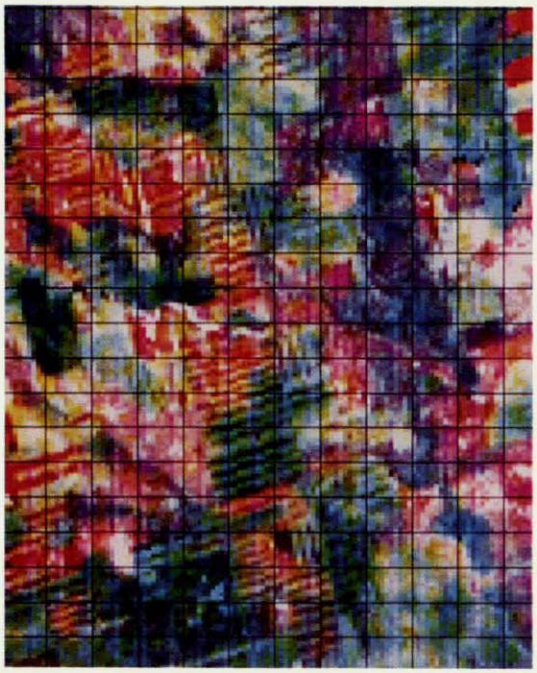

(a) Segment 1739 Acquisition 77114 PRC 19

(c) Segment 1739 Acquisition 77150 PRC 19

Figure 4.15

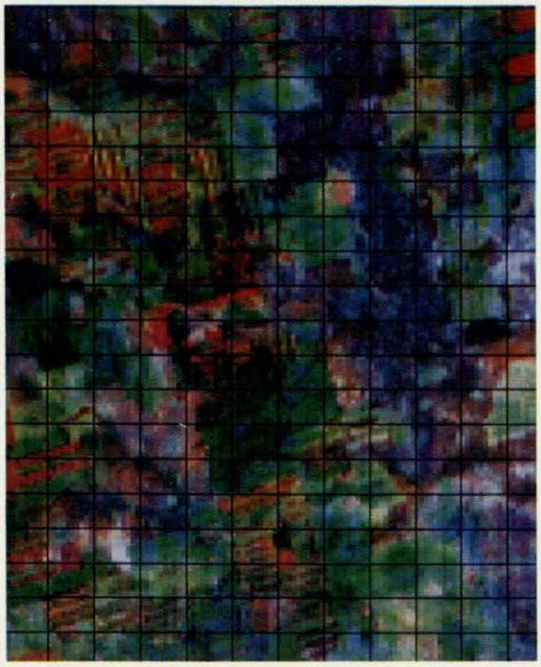

(b) Segment 1739 Acquisition 77132 PRC 20

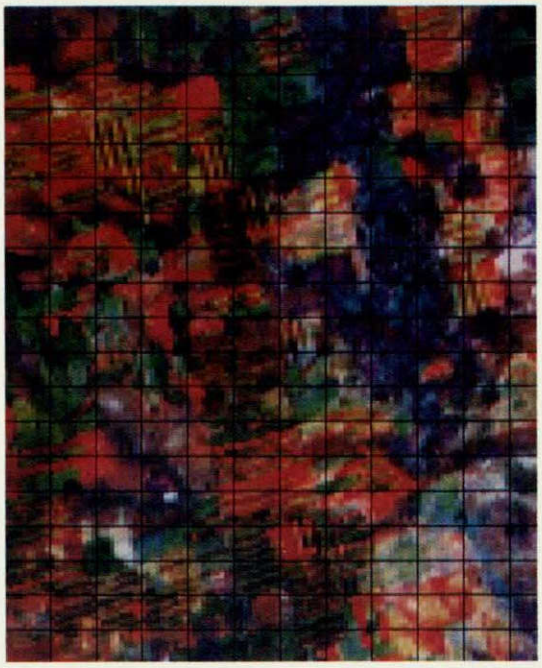

(d) Segment 1739 Acquisition 77168 PRC 20

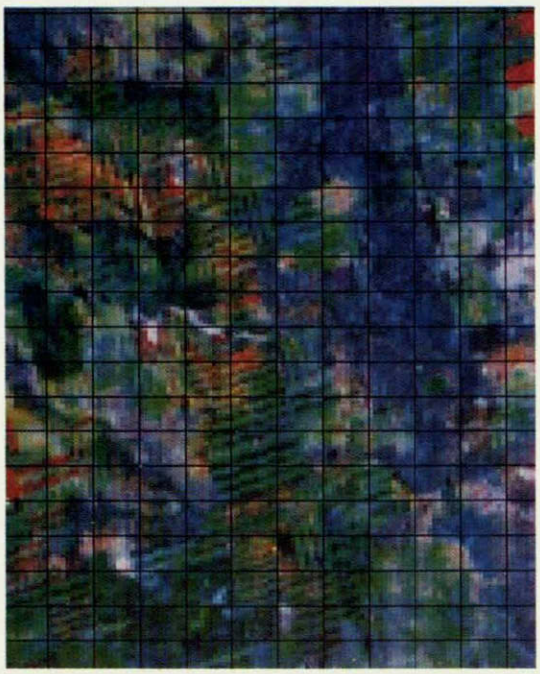

(a) Segment 1739 Acquisition 77114 PRC 20

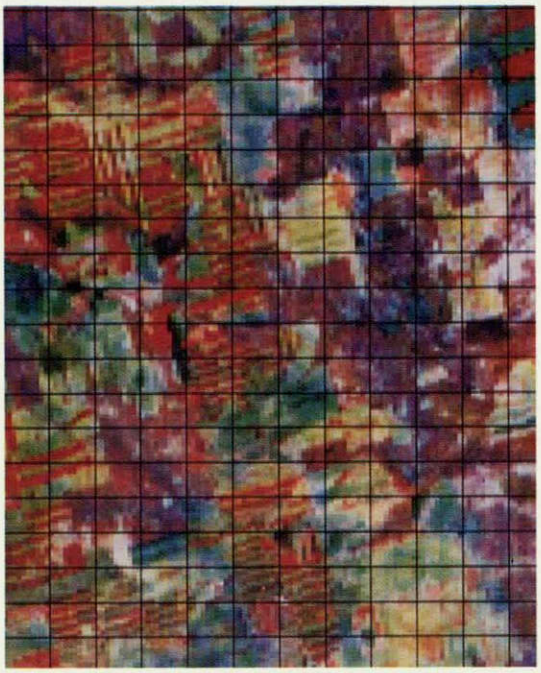

(c) Segment 1739 Acquisition 77150 PRC 20

Figure 4.16

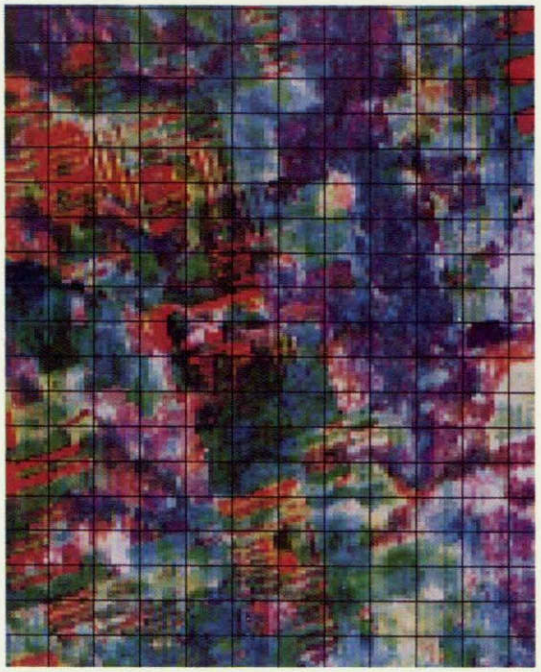

(b) Segment 1739 Acquisition 77132 PRC 21

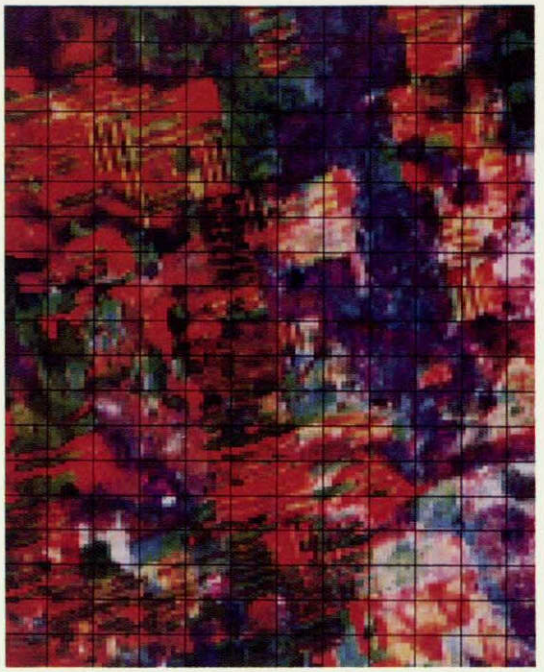

(d) Segment 1739 Acquisition 77168 PRC 21

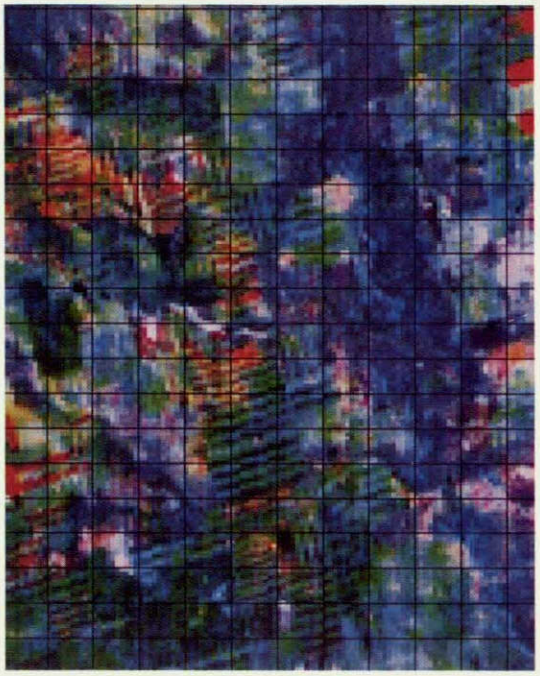

(a) Segment 1739 Acquisition 77114 PRC 21

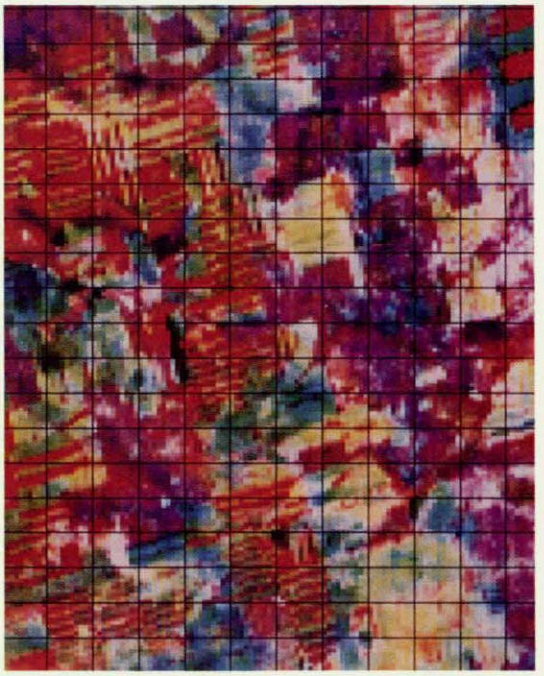

(c) Segment 1739 Acquisition 77150 PRC 21

Figure 4.17

5. SUMMARY AND CONCLUSION

For comparison purposes, IPL equivalents of LACIE products 1 and 3 were created for all acquisitions of the working data set. Twenty-two separate new products were created, all of which utilized forward and reverse principal component transformations. The problem of accentuated color speckle seemed best dealt with by performing two dimensional median filtering on the lower order principal components before the reverse transformation was applied. There appeared to be little difference in the end products between the input of MSS 4, 5, 6, and 7, and MSS 4, 5, and 7 into the principal component transformation color enhancement process, so MSS 4, 5, and 7 were used almost exclusively. There also appeared to be little difference between the two types of variance equalization utilized in the principal component domain. Where there were differences, the linear variance equalization method seemed better than the Gaussian variance equalization method.

Although the principal component transformation color enhancement technique dramatically increased the color range, individual colors retained their basic character and were not transformed to totally different regions of the color spectrum. Strict color consistency coupled with color expansion was enforced over all the acquisitions within a given segment through the use of merged data sets in the generation of the principal component transformation and variance equalization parameters. The initial processing produced color products of low contrast which was attributed to the disjointedness of the individual acquisition data histograms. A sun angle and atmospheric path length correction was applied to the individual acquisitions in an attempt to tighten up the merged data set distributions before the principal component transformation was performed. The end products seemed to show that while some segments yielded promising results, the individual acquisition data histograms were still too disjoint in other segments. Unnormalized variations due to atmospheric haze remained, and may be the source of the difficulty.

In general, greater color discriminability could be obtained through the use of the principal component transformation color enhancement process. Such processing seems to show promise, especially in terms of multicrop analysis where the greater obtainable color range may make the distinction between different crops more pronounced.

6. APPENDICES

6.1 TWO DIMENSIONAL MEDIAN AND MODE FILTERS

The two dimensional median filter is an nxm box filter which replaces the center element of the box with the median of the distribution of all the elements in the box. For example, if a 3x3 median filter is being performed and the elements in the box have the following values:

2	1	2
3	3	3
4	5	4

then the element in the center will remain a 3. If the element in the lower right corner were changed to a 10, the element in the center would still remain a 3 after the filter was performed. In this way, high frequency information is removed while low frequency information is preserved. However, if a feature edge is encountered, the median value of the box will change abruptly as the box moves across the edge, hence preserving the high frequency information related to the edge. In this manner, the high frequency information related to speckle can be suppressed while that relating to feature edges can be preserved.

The two dimensional mode filter is an nxm box filter which replaces the center element of the box with the mode of the distribution of all elements in the box. If a 3x3 mode filter is being applied to the following box:

7	2	4
1	1	6
5	8	1

then the center element would not be changed. The corresponding median filter would change the center element to a 4.

6.2 SUNANGLE AND ATMOSPHERIC PATH LENGTH CORRECTIONS

To correct for differences in solar illumination angle and corresponding atmospheric path length, the data under consideration was multiplied by a factor which normalized the effective incident radiation to a sunangle of 90° and hence an atmospheric path length of one. The corrections for sunangle and atmospheric path length were determined separately and then multiplied together to give the total correction factor. The assumption made in this correction was that the observed brightness is directly proportional to the incident radiance. To

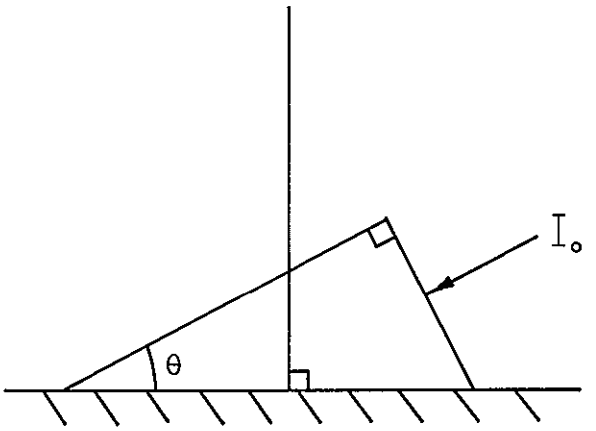

FIGURE 6.2.1 Solar illumination geometry

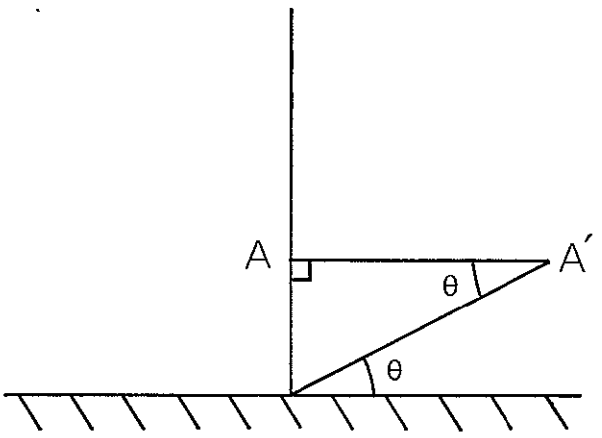

FIGURE 6.2.2 Atmospheric path geometry

TABLE 6.2.1

SUNANGLE AND ATMOSPHERIC PATH
LENGTH CORRECTIONS FOR SEGMENT 1739

ACQUISITION	MSS	SUNANGLE	SUNANGLE CORRECTION	PATH LENGTH CORRECTION	TOTAL CORRECTION
76282	4	31	1.94	1.09	2.11
	5	31	1.94	1.05	2.04
	6	31	1.94	1.03	2.00
	7	31	1.94	1.01	1.96
77114	4	46	1.39	1.04	1.45
	5	46	1.39	1.02	1.42
	6	46	1.39	1.01	1.40
	7	46	1.39	1.01	1.40
77132	4	51	1.29	1.03	1.33
	5	51	1.29	1.01	1.30
	6	51	1.29	1.01	1.30
	7	51	1.29	1.00	1.29
77150	4	53	1.25	1.02	1.28
	5	53	1.25	1.01	1.26
	6	53	1.25	1.01	1.26
	7	53	1.25	1.00	1.25
77168	4	54	1.24	1.02	1.26
	5	54	1.24	1.01	1.25
	6	54	1.24	1.01	1.25
	7	54	1.24	1.00	1.24
77222	4	47	1.37	1.03	1.41
	5	47	1.37	1.02	1.40
	6	47	1.37	1.01	1.38
	7	47	1.37	1.00	1.37

determine the sunangle correction consider the diagram of Figure 6.2.1. If θ is the solar elevation angle and I_o is the solar radiance, then the actual energy per unit area radiating the surface is $I_o \sin \theta$. Therefore to correct to a sunangle of 90°, the observed brightness values need to be multiplied by $1/\sin \theta$.

From Kondratyev (Ref. 8, p. 162), the atmospheric path length can be used to calculate the atmospheric mass m by taking the ratio of the path length at the given sunangle to the path length in the vertical direction as shown in the Figure 6.2.2. If the top of the atmosphere is AA′ (assumed to be flat) then $m = 1/\sin \theta$. Using this result and a table of energy distributions in the solar spectrum for different atmospheric mass (Ref. 8, p. 222), a correction could be determined to normalize the effective path length to a sunangle of 90°. This was done for each of MSS 4,5,6,7.

The two correction terms were multiplied together to give the total correction factor. Table 6.2.1 lists the correction factors applied to all the acquisitions for segment 1739.

6.3 ASSESSMENT OF NORMALIZATION RESULTS

The degree to which the composite distribution (in histogram space) is tightened, relative to the distributions of the individual acquisitions, provides an approach for evaluating the success of the normalization. To perform the assessment, the means of all of the bands for each of the acquisitions in the given segment may be examined before and after the normalization is applied. In order to represent the distribution of these means, a mean and standard deviation of the means themselves was calculated for each band. Let μ_{ik} be the mean for band i of acquisition k. Then

$$m_i = \frac{1}{n} \sum_{k=1}^{n} \mu_{ik} \; ; \; s_i^2 = \frac{1}{n} \sum_{k=1}^{n} (\mu_{ik} - m_i)^2$$

where n is the number of acquisitions in the given segment. Since all of the correction factors are greater than unity, the distribution of the post-normalization means may have a larger variance than the pre-normalization means, but in fact be relatively closer together. To account for this, a measure of the relative change in the distribution of the acquisition means may be obtained by calculating a relative standard deviation by taking the ratio (s_i/m_i) before and after normalization. Further, to make the effects of normalization more readily

apparent, the ratio of the relative standard deviations may be calculated as follows:

$$R_i = \frac{\left(\frac{s_i}{m_i}\right)_{\text{post-normalization}}}{\left(\frac{s_i}{m_i}\right)_{\text{pre-normalization}}}$$

Therefore, if R_i is less than 1, the distribution of acquisition means in band i has been tightened as a result of the normalization process.

Table 6.3.1 displays the above quantities for all the segments of the working data set except segments 1531, 9930 and 9931. (The solar elevation values for these three segments were incorrect.) Using segment 1739 as a rough guide, inspection of the table shows that only about half of the segments showed promise using this technique. One may attribute part of the lack of complete success to other external influences such as atmospheric haze, whose effects are more difficult to determine. On the other hand, if the acquisition data distributions are in reality sufficiently disjointed, then the modelling performed here should not be expected to merge the individual distributions. When this is the case, a subset of the acquisitions under consideration might be chosen to yield better results.

TABLE 6.3.1

RELATIVE CHANGE IN THE DISTRIBUTION OF ACQUISITION MEANS
AS A RESULT OF SUNANGLE AND ATMOSPHERIC PATH LENGTH NORMALIZATION

SEGMENT NO.	BAND	PRE-NORM. s_i/m_i	POST-NORM. s_i/m_i	R_i
1000	4	0.35	0.12	0.34
	5	0.34	0.12	0.35
	6	0.35	0.08	0.23
	7	0.31	0.05	0.16
1183	4	0.28	0.14	0.50
	5	0.23	0.20	0.87
	6	0.43	0.15	0.35
	7	0.39	0.12	0.31
1531	4	0.22	0.10	0.45
	5	0.21	0.12	0.57
	6	0.27	0.08	0.30
	7	0.26	0.07	0.27
1606	4	0.15	0.10	0.67
	5	0.16	0.13	0.81
	6	0.22	0.15	0.68
	7	0.23	0.16	0.70
1625	4	0.12	0.13	1.08
	5	0.17	0.20	1.18
	6	0.10	0.06	0.60
	7	0.11	0.06	0.55
1637	4	0.16	0.11	0.69
	5	0.18	0.16	0.89
	6	0.23	0.17	0.74
	7	0.27	0.21	0.78
1648	4	0.19	0.18	0.95
	5	0.19	0.18	0.95
	6	0.17	0.13	0.76
	7	0.18	0.13	0.72
1734	4	0.25	0.08	0.32
	5	0.25	0.08	0.32
	6	0.26	0.11	0.42
	7	0.23	0.08	0.35
1739	4	0.15	0.05	0.33
	5	0.13	0.07	0.54
	6	0.18	0.06	0.33
	7	0.17	0.05	0.29

7. REFERENCES

1. Taylor, M.M., "Principal Components Colour Display of ERTS Imagery", Third Earth Resources Technology Satellite-1 Symposium, NASA SP-351, pp. 1877-1897, December 10-14, 1973.

2. Soha, J.M. and A.A. Schwartz, "Multispectral Histogram Normalization Contrast Enhancement", Proceedings of the Fifth Canadian Symposium on Remote Sensing, August, 1978.

3. Kauth, R.J. and G.S. Thomas, "The Tasselled Cap-A Graphic Description of the Spectral-Temporal Development of Agricultural Crops as Seen by Landsat", Proceedings of the Symposium on Machine Processing of Remotely Sensed Data, Purdue, June, 1976.

4. Juday, R.D. and R.A. Abotteen, "A Maximal Chromatic Expansion Method of Mapping Multichannel Imagery into Color Space", Technical Report LEC-10830 prepared by Lockheed Electronics Company, Inc., Systems and Services Division, Houston, Texas, under Contract NAS 9-15200 for Earth Observations Division, Space and Life Sciences Directorate, NASA, Lyndon B. Johnson Space Center, Houston, Texas, January, 1978.

5. Ready, P.J. and P.A. Wintz, "Information Extraction, SNR Improvement, and Data Compression in Multispectral Imagery", IEEE Trans. on Communications, Vol. COM-21, No. 10, pp. 1123-1121, October, 1973.

6. Pratt, W.K., Digital Image Processing, Section 12.6, John Wiley and Sons, Inc., New York, Copyright 1978.

7. Austin, W.W., "Detailed Description of the Wheat Acreage Estimation Procedure Used in the Large Area Crop Inventory Experiment", Technical Memorandum LEC-11497, Lockheed Electronics Company, Inc., Aerospace Systems Division, Houston, Texas, February, 1978.

8. Kondratyev, K. YA., Radiation in the Atmosphere, Academic Press, Inc., New York, Copyright 1969.

NASA—JPL—Coml, LA, Calif

jpl → PUBLICATION 78-102